

1 **SYNERGY BETWEEN SATELLITE OBSERVATIONS OF SOIL MOISTURE**  
2 **AND WATER STORAGE ANOMALIES FOR RUNOFF ESTIMATION**

3 Stefania Camici <sup>(1)</sup>, Gabriele Giuliani <sup>(1)</sup>, Luca Brocca <sup>(1)</sup>, Christian Massari <sup>(1)</sup>, Angelica Tarpanelli  
4 <sup>(1)</sup>, Hassan Hashemi Farahani <sup>(2)</sup>, Nico Sneeuw <sup>(2)</sup>, Marco Restano <sup>(3)</sup>, Jérôme Benveniste <sup>(4)</sup>

5 *(1) National Research Council, Research Institute for Geo-Hydrological Protection, Perugia, Italy ([s.camici@irpi.cnr.it](mailto:s.camici@irpi.cnr.it))*

6 *(2) Institute of Geodesy, University of Stuttgart, Geschwister-Scholl-Straße 24D, 70174 Stuttgart, Germany*

7 *(3) SERCO c/o ESA-ESRIN, Largo Galileo Galilei, Frascati, 00044, Italy*

8 *(4) European Space Agency, ESA-ESRIN, Largo Galileo Galilei, Frascati, 00044, Italy*

9

10

11

12

13

14

15

16

17

18

**November 2020**

19

Submitted to:

20

\* Correspondence to: Ph.D. Stefania Camici, Research Institute for Geo-Hydrological Protection, National Research Council, Via della Madonna Alta 126, 06128 Perugia, Italy. Tel: +39 0755014419 Fax: +39 0755014420 E-mail: [stefania.camici@irpi.cnr.it](mailto:stefania.camici@irpi.cnr.it).

## 21    **ABSTRACT**

22    This paper presents an innovative approach, STREAM - SaTellite based Runoff Evaluation And  
23    Mapping - to derive daily river discharge and runoff estimates from satellite soil moisture,  
24    precipitation and terrestrial water storage anomalies observations. Within a very simple model  
25    structure, the first two variables (precipitation and soil moisture) are used to estimate the quick-flow  
26    river discharge component while the terrestrial water storage anomalies are used for obtaining its  
27    complementary part, i.e., the slow-flow river discharge component. The two are then summed up to  
28    obtain river discharge and runoff estimates.

29    The method is tested over the Mississippi river basin for the period 2003-2016 by using Tropical  
30    Rainfall Measuring Mission (TRMM) Multi-satellite Precipitation Analysis (TMPA) precipitation  
31    data, European Space Agency Climate Change Initiative (ESA CCI) soil moisture data and Gravity  
32    Recovery and Climate Experiment (GRACE) terrestrial water storage data. Despite the model  
33    simplicity, relatively high-performance scores are obtained in river discharge simulations, with a  
34    Kling-Gupta efficiency index greater than 0.65 both at the outlet and over several inner stations used  
35    for model calibration highlighting the high information content of satellite observations on surface  
36    processes. Potentially useful for multiple operational and scientific applications (from flood warning  
37    systems to the understanding of water cycle), the added-value of the STREAM approach is twofold:  
38    1) a simple modelling framework, potentially suitable for global runoff monitoring, at daily time scale  
39    when forced with satellite observations only, 2) increased knowledge on the natural processes, human  
40    activities and on their interactions on the land.

41

42    Key words: satellite products, soil moisture, water storage variations, conceptual hydrological  
43    modelling, rainfall-runoff modelling, Mississippi.

## 44 1. INTRODUCTION

45 Spatial and temporal continuous river discharge monitoring is paramount for improving the  
46 understanding of the hydrological cycle, for planning human activities related to water use as well as  
47 to prevent/mitigate the losses due to extreme flood events. To accomplish these tasks, runoff and river  
48 discharge data, which represents the aggregated signal of runoff (Fekete et al., 2012), should be  
49 available at adequate spatial/temporal resolution, i.e., at basin scale (basin area larger than 10'000  
50 km<sup>2</sup>) and at monthly time step for water resources management and drought monitoring up to grid  
51 scale (few km)/(sub-) daily time step for flood prediction. The accurate continuous (in space and  
52 time) runoff and river discharge estimation at finer spatial/temporal resolution is still a big challenge  
53 for hydrologists.

54 Traditional in situ observations of river discharge, even if generally characterized by high temporal  
55 resolution (up to sub-hourly time step), typically offer little information on the spatial distribution of  
56 runoff within a watershed. Moreover, river discharge observation networks suffer from many  
57 limitations such as low station density and often incomplete temporal coverage, substantial delay in  
58 data access and large decline in monitoring capacity (Vörösmarty et al. 2002). Paradoxically, this  
59 latter issue is exacerbated in developing nations (Crochemore et al, 2020), where the knowledge of  
60 the terrestrial water dynamics deserves greater attention due to huge damages to settlements and  
61 especially the loss of human lives that occurs regularly.

62 This precarious situation has led to growing interest in finding alternative solutions, i.e., model-based  
63 or observation-based approaches, for runoff and river discharge monitoring. Model-based  
64 approaches, based on the mathematical description of the main hydrological processes (e.g., water  
65 balance models, WBMs, global hydrological models, GHMs, e.g., Döll et al., 2003 or, increasing in  
66 complexity, land surface models, LSM, e.g., Balsamo et al., 2009; Schellekens et al., 2017), are able  
67 to provide comprehensive information on a large number of relevant variables of the hydrological  
68 cycle including runoff and river discharge at very high temporal and spatial resolution (up to hourly

69 sampling and 0.05° grid scale). However, the values of simulated water balance components rely on  
 70 a massive parameterization of the soil, vegetation and land parameters, which is not always realistic,  
 71 and are strongly dependent on the GHM/ LSM models used, analysis periods (Wisser et al., 2010)  
 72 and climate forcings selected (e.g Haddeland et al., 2012; Gudmundsson et al., 2012a, b; Prudhomme  
 73 et al., 2014; Müller Schmied et al., 2016).  
 74 Alternatively, the observation-based approaches exploit machine learning techniques and a  
 75 considerable amount of data to describe the physics of the system (i.e. hydraulic and/or hydrologic  
 76 phenomena, Solomatine and Ostfeld, 2008) with only a limited number of assumptions. Besides being  
 77 simpler than model-based approaches, these approaches still present some limitations. At first, as they  
 78 rely on a considerable amount of data describing the modelled system's physics, the spatial/temporal  
 79 extent and the uncertainty of the resulting dataset is determined by the spatial/temporal coverage and  
 80 the accuracy of the forcing data (e.g., see E-RUN dataset, Gudmundsson and Seneviratne, 2016;  
 81 GRUN dataset, Ghiggi et al., 2019; FLO1K dataset, Barbarossa et al., 2018). Additional limitations  
 82 stem from the employed method to estimate runoff. Indeed, random forests such as employed in  
 83 Gudmundsson and Seneviratne, 2016, like other machine learning techniques, are powerful tools for  
 84 data driven modeling, but they are prone to overfitting, implying that noise in the data can obscure  
 85 possible signals (Hastie et al., 2009). Moreover, the influence of land parameters on continental-scale  
 86 runoff dynamics is not taken into account as the underlying hypothesis is that the hydrological  
 87 response of a basin exclusively depend on present and past atmospheric forcing. It is easy to  
 88 understand that this assumption will only be valid in certain circumstances and might lead to  
 89 problems, e.g., over complex terrain (Orth and Seneviratne, 2015) or in cases of human river flow  
 90 regulation (Ghiggi et al., 2019).  
 91 Remote sensing can provide estimates of nearly all the climate variables of the global hydrological  
 92 cycle including soil moisture (e.g., Wagner et al., 2007; Seneviratne et al., 2010), precipitation  
 93 (Huffman et al., 2014) and total terrestrial water storage (e.g., Houborg et al., 2012; Landerer and  
 94 Swenson, 2012; Famiglietti and Rodell, 2013). It has undeniably changed and improved dramatically

95 the ability to monitor the global water cycle and, hence, runoff. By taking advantage of satellite  
96 information, some studies tried to develop methodologies able to optimally produce multivariable  
97 datasets from the fusion of in situ and satellite-based observations (e.g., Rodell et al., 2015; Zhang et  
98 al., 2018; Pellet et al., 2019). Other studies exploited satellite observations of hydrological variables,  
99 e.g., precipitation (Hong et al., 2007), soil moisture (Massari et al., 2014), and geodetic variables (e.g.,  
100 Sneeuw et al., 2014; Tourian et al., 2018) to monitor single components of the water cycle in an  
101 independent way.

102 Although the majority of these studies provide runoff and river discharge data at basin scale and  
103 monthly time step, they deserve to be recalled here as important for the purpose of the present study.  
104 In particular, Hong et al. (2007) presented a first attempt to obtain an approximate but quasi-global  
105 annual streamflow dataset, by incorporating satellite precipitation data in a relatively simple rainfall-  
106 runoff simulation approach. Driven by the multiyear (1998-2006) Tropical Rainfall Measuring  
107 Mission Multi-satellite Precipitation Analysis, runoff was independently computed for each global  
108 land surface grid cell through the Natural Resources Conservation Service (NRCS) runoff curve  
109 number (CN) method (NRCS, 1986) and subsequently routed to the watershed outlet to simulate  
110 streamflow. The results, compared to the in situ observed discharge data, demonstrated the potential  
111 of using satellite precipitation data for diagnosing river discharge values both at global scale and for  
112 medium to large river basins. If, on the one hand, the work of Hong et al. (2007) can be considered  
113 as a pioneer study, on the other hand it presents a serious drawback within the NRCS-CN method  
114 that lacks a realistic definition of the soil moisture conditions of the catchment before flood events.  
115 This aspect is not negligible, as it is well established that soil moisture is paramount in the partitioning  
116 of precipitation into surface runoff and infiltration inside a catchment (Brocca et al., 2008). In  
117 particular, for the same rainfall amount but different values of initial soil moisture conditions,  
118 different flooding effects can occur (see e.g. Crow et al., 2005; Brocca et al., 2008; Berthet et al.,  
119 2009; Merz and Blochl, 2009; Tramblay et al., 2010). On this line following Brocca et al. (2009),  
120 Massari et al. (2016) presented a very first attempt to estimate global streamflow data by using

121 satellite Soil Moisture Active and Passive (SMAP, Entekhabi et al., 2010) and Global Precipitation  
122 Measurement (GPM, [Huffman et al., 2019](#)) products. Although the validation was carried out by  
123 routing the monthly surface runoff only in a single basin in Central Italy, the obtained results  
124 suggested to dedicate additional efforts in this direction.

125 Among the studies that use satellite observations of hydrological variables for runoff estimation, the  
126 hydro-geodetic approaches are undoubtedly worth mentioning, see e.g., [Sneeuw et al., 2014](#) for a  
127 comprehensive overview or [Lorenz et al. \(2014\)](#) for an analysis of satellite-based water balance  
128 misclosures with discharge as closure term. In particular, the satellite mission Gravity Recovery And  
129 Climate Experiment (GRACE), which observed the temporal changes in the gravity field, has given  
130 a strong impetus to satellite-driven hydrology research ([Tapley et al., 2019](#)). Since temporal gravity  
131 field variations over the continents imply water storage change, GRACE was the first remote sensing  
132 system to provide observational access to deeper groundwater storage. The relation between GRACE  
133 groundwater storage change and runoff was characterized by [Riegger and Tourian \(2014\)](#), which even  
134 allowed the quantification of absolute drainable water storage over the Amazon ([Tourian et al., 2018](#)).

135 In essence the storage-runoff relation describes the gravity-driven drainage of a basin and, hence, the  
136 slow-flow processes. Due to GRACE's spatial-temporal resolution, runoff and river discharge are  
137 generally available for large basins ( $>160'000 \text{ km}^2$ ) and at monthly time step.

138 Based on the above discussion, it is clear that each approach presents strengths and limitations that  
139 enable or hamper the runoff and river discharge monitoring at finer spatial and temporal resolutions.

140 In this context, this study presents an attempt to find an alternative method to derive daily river  
141 discharge and runoff estimates at  $\frac{1}{4}$  degree spatial resolution exploiting satellite observations and the  
142 knowledge of the key mechanisms and processes that act in the formation of runoff, i.e., the role of  
143 soil moisture in determining the response of a catchment to precipitation. For that, soil moisture,  
144 precipitation and terrestrial water storage anomalies (TWSA) observations are used as input into a  
145 simple modelling framework named STREAM v1.3 (SaTellite based Runoff Evaluation And  
146 Mapping, version 1.3). Unlike classical land surface models, STREAM exploits the knowledge of the

147 system states (i.e., soil moisture and TWSA) to derive river discharge and runoff, and thus it 1) skips  
148 the modelling of the evapotranspiration fluxes which are known to be a non-negligible source of  
149 uncertainty (Long et al. 2014), 2) limits the uncertainty associated with the over-parameterization of  
150 soil and land parameters and 3) implicitly takes into account processes, mainly human-driven (e.g.,  
151 irrigation, change in the land use), that might have a large impact on the hydrological cycle and hence  
152 on runoff.

153 The detailed description of the STREAM v1.3 model is given in section 4. The collected datasets and  
154 the experimental design for the Mississippi River Basin (section 2) are described in sections 3 and 5,  
155 respectively. Results, discussion and conclusions are drawn in section 6, 7 and 8, respectively.

## 156 **2. STUDY AREA**

157 The STREAM v1.3 model presented here has been tested and validated over the Mississippi River  
158 basin. With a drainage area of about 3.3 million km<sup>2</sup>, the Mississippi River basin is the fourth largest  
159 watershed in the world, bordered to the West by the crest of the Rocky Mountains and to the East by  
160 the crest of the Appalachian Mountains. According to the Köppen climate classification, the climate  
161 is subtropical humid over the southern part of the basin, continental humid with hot summer over the  
162 central part, continental humid with warm summer over the eastern and northern parts, whereas a  
163 semiarid cold climate affects the western part. The average annual air temperature across the  
164 watershed ranges from 4°C in the West to 6°C in the East. On average, the watershed receives about  
165 900 mm/year of precipitation (77% as rainfall and 23% as snowfall), more concentrated in the eastern  
166 and southern portions of the basin with respect to its northern and western part (Vose et al., 2014).

167 The river flow has a clear natural seasonality mainly controlled by spring snowmelt (coming from  
168 the Missouri and the Upper Mississippi, the eastern and the upper part of the basin, respectively, Dyer  
169 2008) and by heavy precipitation exceeding the soil moisture storage capacity (mostly occurring in  
170 the eastern and southern part of the basin, Berghuijs et al., 2016). The basin is also heavily regulated  
171 by the presence of large dams (Global Reservoir and Dam Database GRanD, Lehner et al., 2011)

most of them located on the Missouri river, over the Great Plains. In particular, the river reach between Garrison and Gavins Point dams is the portion of the Missouri river where the large main-channel dams have the greatest impact on river discharge providing a substantial reduction in the annual peak floods, an increase on low flows and a reduction on the overall variability of intra-annual discharges (Alexander et al., 2012). The annual average of Mississippi river discharge at the Vicksburg outlet section is equal to  $17'500 \text{ m}^3/\text{s}$  (see Table 1). Given the variety of climate and topography across the Mississippi River basin, it is a good candidate to test the suitability of the STREAM v1.3 model for river discharge and runoff simulation.

### 3. DATASETS

The datasets used in this study include in situ observations, satellite products and model outputs. The first two datasets have been used as input data to the STREAM v1.3 model. Conversely, the model outputs are used as a benchmark to validate the performance of the STREAM v1.3 model.

#### 3.1 In situ Observations

In situ observations comprise air temperature ( $T_{\text{air}}$ ) and river discharge data ( $Q$ ). For  $T_{\text{air}}$  data the Climate Prediction Center (CPC) Global Temperature data developed by the American National Oceanic and Atmospheric Administration (NOAA) using the optimal interpolation of quality-controlled gauge records of the Global Telecommunication System (GTS) network (Fan et al., 2008) have been used. The dataset, downloadable at (<https://psl.noaa.gov/data/gridded/data.cpc.globaltemp.html>) is available on a global regular  $0.5^\circ \times 0.5^\circ$  grid, and provides daily maximum ( $T_{\text{max}}$ ) and minimum ( $T_{\text{min}}$ ) air temperature data from 1979 to present. The daily average air temperature data have been generated as the mean of  $T_{\text{max}}$  and  $T_{\text{min}}$  of each day.

Daily  $Q$  data over the study basins have been taken from the Global Runoff Data Center (GRDC, [https://www.bafg.de/GRDC/EN/Home/homepage\\_node.html](https://www.bafg.de/GRDC/EN/Home/homepage_node.html)). In particular, 11 gauging stations located along the main river network of the Mississippi River basin have been selected to represent



the spatial distribution of runoff over the basin. The location of these gauging stations along with relevant characteristics (e.g., the upstream basin area, the mean annual river discharge and the presence of upstream dams) are summarized in Table 1. As it can be noted, mean annual river discharge ranges from 141 to 17'500 m<sup>3</sup>/s, and 3 out 11 sections are located downstream big dams (Lehner et al., 2011). In particular, Garrison (the fifth-largest earthen dam in the world), Gavins Point and Kanopolis dams located downstream section 1, 2 and 5 respectively (see Figure 3 and Table 1), are three large dams with a maximum storage of 29'383×10<sup>9</sup> m<sup>3</sup>, 0.607×10<sup>9</sup> m<sup>3</sup>, and 1.058×10<sup>9</sup> m<sup>3</sup> respectively.

### 3.2 Satellite Products

Satellite products include observations of precipitation (*P*), soil moisture and TWSA. The satellite *P* dataset used in this study is the Multi-satellite Precipitation Analysis 3B42 Version 7 (TMPA 3B42 V7) estimate produced by the National Aeronautics and Space Administration (NASA) as the 0.25°×0.25° quasi-global (50°N-S) gridded dataset. The TMPA 3B42 V7 is a gauged-corrected satellite product, with a latency period of two months after the end of the month of record, available at 3h sampling interval from 1998 to present (2020). Major details about the *P* dataset, downloadable from <http://pmm.nasa.gov/data-access/downloads/trmm>, can be found in Huffman et al. (2007). Soil moisture data have been taken from the European Space Agency Climate Change Initiative (ESA CCI) Soil Moisture project (<https://esa-soilmoisture-cci.org/>) that provides a surface soil moisture product (referred to first 2-3 centimeters of soil) continuously updated in term of spatial-temporal coverage, sensors and retrieval algorithms (Dorigo et al., 2017). In this study, the daily combined ESA CCI soil moisture product v4.2 is used, that is available at global scale with a grid spacing of 0.25°, for the period 1978-2016. TWSA have been obtained from the Gravity Recovery And Climate Experiment (GRACE) satellite mission. Here we employ the NASA Goddard Space Flight Center (GSFC) global mascon model, i.e., Release v02.4, (Luthcke et al. 2013). It has been produced based on the mass concentration

(mascon) approach. The model provides surface mass densities on a monthly basis. Each monthly solution represents the average of surface mass densities within the month, referenced at the middle of the corresponding month. The model has been developed directly from GRACE level-1b K-Band Ranging (KBR) data. It is computed and delivered as surface mass densities per patch over blocks of approximately  $1^{\circ} \times 1^{\circ}$  or about 12'000 km<sup>2</sup>. Although the mascon size is smaller than the inherent spatial resolution of GRACE, the model exhibits a relatively high spatial resolution. This is attributed to a statistically optimal Wiener filtering, which uses signal and noise full covariance matrices. This allows the filter to fine tune the smoothing in line with the signal-to-noise ratio in different areas. That is, the less smoothing, the higher signal-to-noise ratio in a particular area and vice versa. This ensures that the filtering is minimal and aggressive smoothing is avoided when unnecessary. Further details of such a filter can be found in Klees et. al (2008). Importantly, the coloured (frequency-dependent) noise characteristic of KBR data was taken in to account when compiling the GRACE model, which has allowed for a reliable computation of the aforementioned noise full covariance matrices. The coloured (frequency-dependent) noise characteristic of KBR data was taken into account when compiling the model, which has allowed for a reliable computation of these noise and signal covariance matrices. They play a crucial role when filtering and allow to achieve a higher spatial resolution compared to commonly applied GRACE filtering methods such as Gaussian smoothing and/or destriping filters. GRACE data are available for the period 01 January 2003 to 15 July 2016.

### 3.3 Model Outputs

To establish the quality of the STREAM v1.3 model in runoff simulation, monthly runoff ( $R$ ) data obtained from the Global Runoff Reconstruction (GRUN\_v1, <https://doi.org/10.3929/ethz-b-000324386>) have been used for comparison. The GRUN dataset (Ghiggi et al., 2019) is a global monthly  $R$  dataset derived through the use of a machine learning algorithm trained with in situ  $Q$  observations of relatively small catchments (<2500 km<sup>2</sup>) and gridded precipitation and temperature

247 derived from the Global Soil Wetness Project Phase 3 (GSWP3) dataset ([Kim et al., 2017](#)). The  
248 dataset covers the period from 1902 to 2014 and it is provided on a  $0.5^\circ \times 0.5^\circ$  regular grid.

## 249 **4. METHOD**

### 250 **4.1 STREAM Model: the Concept**

251 The concept behind the STREAM v1.3 model is that river discharge is a combination of hydrological  
252 responses operating at diverse time scales ([Blöschl et al., 2013](#); [Rakovec et al., 2016](#)). In particular,  
253 river discharge can be considered made up of a *slow-flow component*, produced as outflow of the  
254 groundwater storage and of a *quick-flow component*, i.e. mainly related to the surface and subsurface  
255 runoff components ([Hu and Li, 2018](#)).

256 While the high spatial and temporal (i.e., intermittence) variability of precipitation and the highly  
257 changing land cover spatial distribution significantly impact the variability of the *quick-flow*  
258 *component* (with scales ranging from hours to days and meters to kilometres depending on the basin  
259 size), *slow-flow river discharge* reacts to precipitation inputs more slowly (i.e., months) as water  
260 infiltrates, is stored, mixed and is eventually released in times spanning from weeks to months.  
261 Therefore, the two components can be estimated by relying upon two different approaches that  
262 involve different types of observations. Based on that, within the STREAM v1.3 model, satellite soil  
263 moisture, precipitation and TWSA will be used for deriving river discharge and runoff estimates. The  
264 first two variables are used as proxy of the *quick-flow* river discharge component while TWSA is  
265 exploited for obtaining its complementary part, i.e., the *slow-flow river discharge* component. Firstly,  
266 we exploit the role of the soil moisture in determining the response of the catchment to the  
267 precipitation inputs, which have been soundly demonstrated in more than ten years of literature  
268 studies (see e.g., [Brocca et al., 2017](#) for a comprehensive discussion on the topic). Secondly, we  
269 consider the important role of terrestrial water storage in determining the slow-flow river discharge  
270 component as modelled in several hydrological models (e.g., [Sneeuw et al., 2014](#)).

271 It is worth noting that this *modus operandi*, i.e. to model the *quick-flow* and *slow-flow* discharge  
272 component separately exploring their process controls independently, has been largely applied and  
273 tested in recent and past studies, e.g., for the estimation of the flow duration curve (see e.g. Botter et  
274 al., 2007a, b; Yokoo and Sivapalan 2011; Muneepeerakul et al., 2010; Ghotbi et al., 2020).

#### 275 **4.2 STREAM Model: the Laws**

276 The STREAM v1.3 model is a conceptual hydrological model that, by using as input observation of  
277  $P$ , soil moisture, TWSA and  $T_{\text{air}}$  data, simulates continuous  $R$  and  $Q$  time series.

278 The model entails three main components (Figure 1): 1) a snow module to separate precipitation into  
279 snowfall and rainfall, 2) a soil module to simulate the evolution in time  $t$  of the quick and slow runoff  
280 responses,  $Q_{fu}$  [mm] and  $Q_{sl}$  [mm], and 3) a routing module that transfers these components through  
281 the basins and the rivers for the simulation of the *quick-flow* river discharge,  $QF$  [m<sup>3</sup>/s], and the *slow-*  
282 *flow* river discharge,  $SF$  [m<sup>3</sup>/s] components. The soil module is composed of two storages,  $Su$  and  $Sl$   
283 as illustrated in Figure 1. The upper storage receives inputs from  $P$ , released through a snow module  
284 (Cislaghi et al., 2020) as rainfall ( $r$ ) or stored as snow water equivalent ( $SWE$ ) within the snowpack  
285 and on the glaciers. In particular, according to Cislaghi et al. (2020),  $SWE$  is modelled by using as  
286 input  $T_{\text{air}}$  and a degree-day coefficient,  $C_m$ , to be estimated by calibration. We have to acknowledge  
287 that, even though this rain/snow differentiation method works quite efficiently at a large grid size like  
288 the one used in the study (25 x 25 km), the topographic complexity of higher elevations can be lost.  
289 A different differentiation scheme based e.g., on the wet bulb temperature like in IMERG (Wang et  
290 al., 2019; Arabzadeh and Behrangi, 2021), would be preferable but is out of the purpose study.

291 Once separated,  $r$  input contributes to the quick runoff response while the  $SWE$  (like other fluxes  
292 contributing to modify the soil water content into  $Su$ ) is neglected as already considered in the satellite  
293 TWSA. Therefore, the first key point of the STREAM v1.3 model is that the water content in the  
294 upper storage is directly provided by the satellite soil moisture observations and the loss processes  
295 like infiltration or evaporation do not need to be explicitly modelled to simulate the evolution in time

296  $t$  of soil moisture. Consequently, the quick runoff response,  $Qfu$  from the first storage can be  
 297 computed following the formulation proposed by Georgakakos and Baumer (1996), as in equation  
 298 (1):

$$299 \quad Qfu(t) = r(t) SWI(t, T)^\alpha \quad (1)$$

300 where:

301 -  $SWI$  is the Soil Water Index (Wagner et al., 1999), i.e., the root-zone soil moisture product referred  
 302 to the first layer of the model (representative of the first 5-30 centimeters of soil), derived by the  
 303 surface satellite soil moisture product,  $\theta$ , by applying the exponential filtering approach in its  
 304 recursive formulation (Albergel et al., 2009):

$$305 \quad SWI_n = SWI_{n-1} + K_n(\theta(t_n) - SWI_{n-1}) \quad (2)$$

306 with the gain  $K_n$  at the time  $t_n$  given by:

$$307 \quad K_n = \frac{K_{n-1}}{K_{n-1} + e^{\left(\frac{t_n - t_{n-1}}{T}\right)}} \quad (3)$$

- 308 -  $T$  [days] is a parameter, named characteristic time length, that characterizes the temporal variation
- 309 of soil moisture within the root-zone profile and the gain  $K_n$  ranges between 0 and 1;
- 310 -  $\alpha$ [-] is a coefficient linked to the non-linearity of the infiltration process and it takes into account
- 311 the characteristics of the soil;
- 312 - for the initialization of the filter  $K_1 = 1$  and  $SWI_1 = \theta(t_1)$ .

313 The second key point of STREAM v1.3 model concerns the estimation of the slow runoff response,  
 314  $Qsl$ , from the second storage. The hypothesis here, shared also with other studies (e.g., Rakovec et al.,  
 315 2016), is that the dynamic of the slow runoff component can be represented by the monthly TWSA  
 316 data. Indeed, the time scale of slow runoff response is typically in the range of seasons to years and it  
 317 can be assumed almost independent upon the water that is contained in that upper storage. For that, the

slow runoff response  $Q_{sl}$ , from the second storage, can be computed following the formulation proposed by Famiglietti and Wood (1994), through equation (4) as follows:

$$Q_{sl}(t) = \beta (TWSA^*(t))^m \quad (4)$$

where:

- $TWSA^*$  [-] is the TWSA estimated by GRACE normalized by its minimum and maximum values. The assumption behind this equation is that TWSA can be assumed as a proxy of the evolution in time,  $t$ , of the  $Sl$ , i.e., the storage of the lower storage.
- $\beta$  [mm h<sup>-1</sup>] and  $m$  [-] are two parameters describing the nonlinearity between slow runoff component and  $TWSA^*$ .

Note that we made the hypothesis that soil moisture and TWSA observations are independent (whereas in the reality soil moisture can be responsible both for the generation of the quick flow part (mainly) and for the slow flow contribution) given the different temporal (and spatial) scales at which the quick and slow runoff responses act.

The STREAM v1.3 model runs in a semi-distributed version in which the catchment is divided into  $s$  elements, each one representing either a subcatchment with outlet along the main channel or an area draining directly into the main channel. Each element is assumed homogeneous and hence constitutes a lumped system.

The routing module (controlled by a  $\gamma$  parameter) conveys the  $Q_{fu}$  and  $Q_{sl}$  response components at each element outlet (subcatchments and directly draining areas, [Brocca et al., 2011](#)) and successively at the catchment outlet of the basin. Specifically, the quick component  $Q_{fu}$  is routed to the element outlet by the Geomorphological Instantaneous Unit Hydro-graph (GIUH, [Gupta et al., 1980](#)) for subcatchments or through a linear reservoir approach ([Nash, 1957](#)) for directly draining areas; the  $Q_{sl}$  slow component is transferred to the outlet section by a linear reservoir approach. Finally, a diffusive linear approach (controlled by the parameters  $C$  and  $D$ , i.e., Celerity and Diffusivity,

342 Troutman and Karlinger, 1985) is applied to route the quick and slow runoff components at the outlet  
343 section of the catchment (Brocca et al., 2011). In the first case we obtain the *quick-flow* river discharge  
344 component,  $QF$  [ $m^3/s$ ], and in the second case the *slow-flow* river discharge component,  $SF$  [ $m^3/s$ ]  
345 (see Figure 1).

#### 346 **4.3 STREAM Parameters**

347 The STREAM v1.3 model uses 8 parameters of which 5 are used in the soil module ( $\alpha$ ,  $T$  [days],  $\beta$   
348 [ $mm\ h^{-1}$ ],  $m$ ,  $C_m$ ) and 3 in the routing module ( $\gamma$ ,  $C$  [ $km\ h^{-1}$ ] and  $D$  [ $km^2\ h^{-1}$ ]). The parameter values,  
349 determined within the feasible parameter space (See Table Appendix A for more details), are  
350 calibrated by maximizing the Kling-Gupta Efficiency index (KGE, Gupta et al., 2009; Kling et al.,  
351 2012, see paragraph 5.1 for more details) between observed and simulated river discharge. For model  
352 calibration, a standard gradient-based automatic optimisation method (Bober 2013) was used.

### 353 **5. EXPERIMENTAL DESIGN**

#### 354 **5.1 Modelling Setup for Mississippi River Basin**

355 The modelling setup is carried out in three steps (Figure 2):

356 1. *Sub-basin delineation*. STREAM v1.3 model is run in the semi-distributed version over the  
357 Mississippi River basin. The TopoToolbox (<https://topotoolbox.wordpress.com/>), a tool developed in  
358 Matlab by Schwanghart et al. (2010), and the SHuttle Elevation Derivatives at multiple Scales  
359 (HydroSHED, <https://www.hydrosheds.org/>) DEM of the basin at the 3'' resolution (nearly 90 m at  
360 the equator) have been used to derive flow directions, to extract the stream network and to delineate  
361 the drainage basins over the Mississippi River basin. In particular, by considering only rivers with  
362 order greater than 3 (according to the Horton-Strahler rules, Horton, 1945; Strahler, 1952), the  
363 Mississippi watershed has been divided into 53 sub-basins as illustrated in Figure 3. Red dots in the  
364 figure indicate the location of the 11 discharge gauging stations selected for the study area.

365 It has to be specified that the step of sub-basin delineation could be accomplished through tools  
366 different from the TopoToolbox. For instance, it could be used the free Qgis software downloadable  
367 at <https://www.qgis.org/it/site/forusers/download.html>, following the instruction to perform the  
368 hydrological analysis as in  
369 [https://docs.qgis.org/3.16/en/docs/training\\_manual/processing/hydro.html?highlight=hydrological%](https://docs.qgis.org/3.16/en/docs/training_manual/processing/hydro.html?highlight=hydrological%20analysis)  
370 [20analysis](https://docs.qgis.org/3.16/en/docs/training_manual/processing/hydro.html?highlight=hydrological%20analysis).

371 2. *Extraction of input data.* Precipitation,  $T_{air}$ , soil moisture and TWSA datasets data have to be  
372 extracted for each sub-basin of the study area. If characterized by different spatial/temporal  
373 resolution, these datasets need to be resampled over a common spatial grid/temporal time step prior  
374 to be used as input into the model.

375 To run the STREAM v1.3 model over the Mississippi river basin, input data have been resampled  
376 over the precipitation spatial grid at  $0.25^\circ$  resolution through a bilinear interpolation. Concerning the  
377 temporal scale,  $T_{air}$ , soil moisture and precipitation data are available at daily time step, while monthly  
378 TWSA data have been linearly interpolated at daily time step. For each of the 53 Mississippi  
379 subbasins, the resampled precipitation, soil moisture,  $T_{air}$  and TWSA data have been extracted.

380 3. *STREAM model calibration.* In situ river discharge data are used as reference data for the  
381 calibration of STREAM v1.3 model. For Mississippi, the STREAM v1.3 model has been calibrated  
382 over five sections as illustrated in Figure 3: the inner sections 4, 6, 9, 11 and the outlet section 10, are  
383 used to calibrate the model and all sub-basins contributing to the respective sections are highlighted  
384 with the same colour. This means that, for example, the sub-basins labelled as 1, 2, 5 to 15, 17, 22,  
385 23, and 30 contribute to section 4, sub-basins 31, 37, 38 and 41 contribute to section 6 and so on.  
386 Consequently, the sub-basins highlighted with the same colour are assigned the same model  
387 parameters, i.e. the parameters that allow to reproduce the river discharge data observed at the related  
388 outlet section.

389 Once calibrated, the STREAM v1.3 model has been run to provide continuous daily Q and R time  
390 series, at the outlet section of each subbasin and over each grid pixel, respectively. By considering



391 the spatial/temporal availability of both in situ and satellite observations, the entire analysis period  
392 covers the maximum common observation period, i.e., from 01 January 2003 to 15 July 2016 at daily  
393 time scale. To establish the goodness-of-fit of the model, the simulated river discharge and runoff  
394 timeseries are compared against in situ river discharge and modelled runoff data.

## 395 **5.2 Model Evaluation Criteria and Performance Metrics**

396 The model has been run over a 13.5-year period split into two sub periods: the first 8 years, from  
397 January 2003 to December 2010, have been used to calibrate the model successively validated over  
398 the remaining 5.5 years (January 2011 - July 2016).

399 In particular, three different validation schemes have been adopted to assess the robustness of the  
400 STREAM v1.3 model:

- 401 1. Internal validation aimed to test the plausibility of both the model structure and the parameter  
402 set in providing reliable estimates of the hydrological variables against which the model is  
403 calibrated. For this purpose, a comparison between observed and simulated river discharge  
404 time series on the sections used for model calibration has been carried out for both the  
405 calibration and validation sub periods.
- 406 2. Cross-validation testing the goodness of the model structure and the calibrated model  
407 parameters to predict hydrological variables at locations not considered in the calibration  
408 phase. In this respect, the cross-validation has been carried out by comparing observed and  
409 simulated river discharge time series in gauged basins not considered during the calibration  
410 phase;
- 411 3. External validation aimed to test the capability of the model “*to get the right answers for the*  
412 *right reasons*” (Kirchner 2006). The rationale behind this concept is that the hydrological  
413 models are today highly performing and able to reproduce a lot of hydrological variables. For  
414 that, the model performances should not only be evaluated against observed streamflow, but  
415 complementary datasets representing internal hydrologic states and fluxes (e.g., soil moisture,  
416 evapotranspiration, runoff etc) should be considered. As runoff is a secondary product of the

STREAM v1.3 model, obtained indirectly from the calibration of the river discharge (basin-integrated runoff), the comparison in terms of runoff can be considered as a further external validation of the model. Runoff, differently from discharge, cannot be directly measured. It is generally modelled through land surface or hydrological models. Its validation requires a comparison against modelled data that, however, suffer from uncertainties (Beck et al., 2017). Based on that, in this study the GRUN runoff dataset described in the section 3.3 has been used for a qualitative comparison.

### 5.3 Performance Metrics

To measure the goodness-of-fit between simulated and observed river discharge data three performance scores have been used:

- the relative root mean square error, RRMSE:

$$RRMSE = \frac{\sqrt{\frac{1}{n} \sum_{i=1}^n (Q_{sim_i} - Q_{obs_i})^2}}{\frac{1}{n} \sum_{i=1}^n (Q_{obs_i})} \quad (5)$$

where  $Q_{obs}$  and  $Q_{sim}$  are the observed and simulated discharge time series of length  $n$ . RRMSE values range from 0 to  $+\infty$ , the lower the RRMSE, the better the agreement between observed and simulated data.

- the Pearson correlation coefficient,  $R$ , measures the linear relationship between two variables:

$$R = \frac{\sum_{i=1}^n (Q_{sim_i} - \overline{Q_{sim}})(Q_{obs_i} - \overline{Q_{obs}})}{\sqrt{\sum_{i=1}^n (Q_{sim_i} - \overline{Q_{sim}})^2 (Q_{obs_i} - \overline{Q_{obs}})^2}} \quad (6)$$

where  $\overline{Q_{obs}}$  and  $\overline{Q_{sim}}$  represent the mean values of  $Q_{obs}$  and  $Q_{sim}$ , respectively. The values of  $R$  range between  $-1$  and  $1$ ; higher values of  $R$  indicate a better agreement between observed and simulated data.

- the Kling-Gupta efficiency index (KGE, Gupta et al., 2009), which provides direct assessment of four aspects of discharge time series, namely shape, timing, water balance and variability. It is defined as follows:

$$KGE = 1 - \sqrt{(R - 1)^2 + (\delta - 1)^2 + (\varepsilon - 1)^2} \quad (7)$$

441 where  $R$  is the correlation coefficient,  $\delta$  the relative variability and  $\varepsilon$  the bias normalized by the  
442 standard deviation between observed and simulated discharge. The KGE values range between  $-\infty$   
443 and 1; the higher the KGE, the better the agreement between observed and simulated data.  
444 Simulations characterized by values of KGE in the range -0.41 and 1 can be assumed as reliable;  
445 values of KGE greater than 0.5 have been assumed good with respect to their ability to reproduce  
446 observed time series (Thiemig et al., 2013).

## 447 **6. RESULTS**

448 The testing and validation of the STREAM v1.3 model is presented and discussed in this section  
449 according to the scheme illustrated in section 5.2.

### 450 **6.1 Internal Validation**

451 The performance of the STREAM v1.3 model over the calibrated river sections is illustrated in Figure  
452 4 and summarized in Table 2. Figure 4 shows observed and simulated river discharge time series over  
453 the whole study period (2003-2016); in Table 2 the performance scores are evaluated separately for  
454 the calibration and validation sub periods. It is worth noting that the model accurately simulates the  
455 observed river discharge data and is able to give the “right answer” with good modelling  
456 performances. Score values of KGE and R over the calibration (validation) period are higher than  
457 0.62 (0.67) and 0.75 (0.75) (resp.) for all the sections; RRMSE is lower than 46% (51%) for all the  
458 sections except for section 9, where it rises up to 71% (77%). The performances remain good even if  
459 they are evaluated over the entire study period as indicated by the scores on the top of each plot of  
460 Figure 4.

### 461 **6.2 Cross-validation**

462 The cross-validation has been carried out over the six river sections illustrated in Figure 5 not used  
463 in the calibration step. The performance scores on the top of each plot refer to the entire study periods;  
464 the scores split for calibration and validation periods are reported in Table 2. For some river sections  
465 the performance is quite low (see, e.g., river section 1, 2 and 5) whereas for others the model is able

466 to simulate the observed discharge data quite accurately (e.g., 7 and 8). In particular, for river sections  
467 1 and 2 even if KGE reaches values equal to 0.35 and 0.40 (for the whole period), respectively, there  
468 is not a good agreement between observed and simulated river discharge and the R score is lower  
469 than 0.55 for both river sections. The worst performance is obtained over section 5, with negative  
470 KGE and low R (high RRSME). These results are certainly influenced by the presence of large dams  
471 located upstream to these river sections (i.e., Garrison, Gavins Point and Kanopolis dams, see Table  
472 1) which have a strong impact on discharge: the model, not having a specific module for modelling  
473 reservoirs, is not able to accurately reproduce the dynamics of river discharge over regulated river  
474 sections. Positive KGE values are obtained over river sections 3, 7 and 8. In particular, over section  
475 3 the STREAM v1.3 model overestimates the observed river discharge due the presence of large dams  
476 along the Missouri river, over the Great Plains region. This area is well known from other large-scale  
477 hydrological models (e. g., ParFlow-CLM and WRF-Hydro) to be an area with very low performances  
478 in terms of river discharge modelling (O'Neill et al., 2020, Tijerina et al., 2021).

479 Over section 7, located over the Rock river, a relatively small tributary of Mississippi river (see Table  
480 1), the STREAM v1.3 model overestimation has to be attributed to: 1) the different characteristics of  
481 the Rock river basin with respect to the entire basin closed to section 6 where the model has been  
482 calibrated (see Figure 3); 2) the small size of the Rock river basin ( $23'000 \text{ km}^2$ , if compared with  
483 GRACE resolution,  $160'000 \text{ km}^2$ ) for which the model accuracy is expect to be lower. Conversely,  
484 the performances over river section 8, whose parameters have been set equal to the ones of river  
485 section 10, are quite high (KGE equal to 0.71, 0.80 and 0.77 for the entire, the calibration and the  
486 validation period, respectively; R equal to 0.83, 0.84 and 0.84 for the entire, calibration and validation  
487 periods, respectively). This outcome demonstrates that under some circumstances, the STREAM v1.3  
488 model can be used to estimate river discharge in basins not calibrated over, especially those without  
489 upstream dams and with comparable size and land cover.

490 Although it is expected that the performances of STREAM v1.3 model, as any hydrological model  
491 calibrated against observed data, can decrease over the gauging sections not used for the calibration,

the findings obtained above raises doubts about the robustness of model parameters and whether it is actually possible to transfer model parameters from one river section to another with different interbasin characteristics. A more in-depth investigation about the model calibration procedure, with special focus on the regionalization of the model parameters, should be carried out but this topic is beyond the scope of the manuscript.

### **6.3 External Validation**

For the external validation, the monthly runoff time series provided by the GRUN datasets have been compared against the ones computed by the STREAM v1.3 model. For that, STREAM daily runoff time series have been aggregated at monthly scale and re-gridded at the same spatial resolution of the GRUN dataset ( $0.5^\circ$ ). The comparison is illustrated in Figure 6 for the common period 2003–2014. Although the two datasets consider different precipitation inputs, the two models agree in identifying two distinct zones in terms of runoff, i.e., the western dry and the eastern wet area. This two distinct zones can be clearly identified also in the GSWP3 and TMPA 3B42 V7 precipitation maps (see Figure S1) used as input in GRUN and STREAM v1.3, respectively, stressing that STREAM runoff output is correctly driven by the input data. However, likely due to the calibration procedure, the STREAM runoff map appears patchier with respect to GRUN and discontinuities along the sub-basin boundaries (identified in Figure 3) can be noted. This should be ascribed to the automatic calibration procedure of the model that, differently from other calibration techniques (e. g., regionalization procedures), does not consider the basin physical attributes like soil, vegetation, and geological properties that govern spatial dynamics of hydrological processes. This calibration procedure can generate sharp discontinuities even for neighbouring subcatchments individually calibrated. It leads to discontinuities in model parameter values and consequently in the simulated hydrological variable (runoff).

## 515 7. DISCUSSION

516 In the previous sections, the ability of the STREAM v1.3 model to accurately simulate river discharge  
517 and runoff time series has been presented. In particular, Figures 4, 5 and 6 demonstrate that satellite  
518 observations of precipitation, soil moisture and terrestrial water storage anomalies can provide  
519 accurate daily river discharge estimates for near-natural large basins (absence of upstream dams), and  
520 for basins with draining area lower than 160'000 km<sup>2</sup> (see section 7), i.e., at spatial/temporal  
521 resolution lower than the ones of the TWSA input data (monthly, 160'000 km<sup>2</sup>). This is an important  
522 result of the study as it demonstrates, on one hand, that the model structure is appropriate with respect  
523 to the data used as input and, on the other hand, the great value of information contained into TWSA  
524 data that, even if characterized by limited spatial/temporal resolution, can be used to simulate runoff  
525 and river discharge at basin scale. This finding has been also confirmed by a preliminary sensitivity  
526 analysis in which the STREAM v1.3 model has been run with different hydrological inputs of  
527 precipitation, soil moisture and total water storage anomaly (not shown here for brevity). In particular,  
528 by running the STREAM v1.3 model with different input configurations (e.g., by using TMPA 3B42  
529 V7 or Climate Prediction Center (CPC) data for precipitation, ESA CCI or Advanced SCATterometer  
530 (ASCAT) data for soil moisture, TWSA or soil moisture data to simulate the slow-flow river  
531 discharge component), we found that STREAM results are more sensitive to soil moisture data rather  
532 than to precipitation input. In addition, by running STREAM v1.3 model with soil moisture data as  
533 input to simulate the slow-flow river discharge component (i.e. without using TWSA data) we found  
534 a deterioration of the model results.

535 Hereinafter, the strengths and the main limitations of the STREAM v1.3 model are discussed.

536 Among the strengths of the STREAM v1.3 model it is worth highlighting:

537 1. **Simplicity.** The STREAM v1.3 model structure: 1) limits the input data required (only  
538 precipitation, air temperature, soil moisture and TWSA data are needed as input; LSM/GHMs require  
539 many additional inputs such as wind speed, shortwave and longwave radiation, pressure and relative

540 humidity); 2) limits and simplifies the processes to be modelled for runoff/discharge simulation.  
541 Processes like evapotranspiration, infiltration or percolation, are not modelled therefore avoiding the  
542 need of using sophisticated and highly parameterized equations (e.g., Penman-Monteith for  
543 evapotranspiration, Allen et al.,1998, Richard equation for infiltration, Richard, 1931); 3) limits the  
544 number of parameters (only 8 parameters have to be calibrated) thus simplifying the calibration  
545 procedure and potentially reduce the model uncertainties related to the estimation of parameter  
546 values.

547 **2. Versatility.** The STREAM v1.3 model is a versatile model suitable for daily runoff and discharge  
548 estimation over sub-basins with different physiographic characteristics. The results obtained in this  
549 study clearly indicate the potential of this approach to be extended at the global scale. Moreover, the  
550 model can be easily adapted to ingest input data with spatial/temporal resolution different from the  
551 one tested in this study (0.25°/daily). For instance, satellite missions with higher space/time  
552 resolution, or near real time satellite products could be considered. As an example, the Next  
553 Generation Gravity Mission design studies all encompass double-pair scenarios, which would greatly  
554 improve upon the current spatial resolution of single-pair missions like GRACE and GRACE-FO (>  
555 100'000 km<sup>2</sup>). The STREAM v1.3 model shows high flexibility also in the possibility to modify the  
556 subbasin delineation and to introduce additional observational river discharge data to be used for the  
557 model calibration.

558 **3. Computationally inexpensive.** Due to its simplicity and the limited number of parameters to be  
559 calibrated, the computational effort for the STREAM v1.3 model is very limited.”

560 However, some limitations have to be acknowledged for the current version of the STREAM v1.3  
561 model:

562 **1. Presence of reservoir, diversion, dams or flood plain.** As the STREAM v1.3 model does not  
563 explicitly consider the presence of discontinuity elements along the river network (e. g, reservoir,  
564 dam or floodplain), discharge estimates obtained for sections located downstream of such elements  
565 might be inaccurate (see, e.g., river sections 1 and 2 in Figure 5).

566 **2. Need of in situ data for model calibration and robustness of model parameters.** As discussed  
567 in the results section, parameter values of the STREAM v1.3 model are set through an automatic  
568 calibration procedure aimed at minimizing the differences between simulated and observed river  
569 discharge. The main drawback of this parameterization technique is that the models parameterized  
570 with this technique may exhibit (1) poor predictability of state variables and fluxes at locations and  
571 periods not considered in the calibration, and (2) sharp discontinuities along sub-basin boundaries in  
572 state flux, and parameter fields (e.g., Merz and Blöschl, 2004). To overcome these issues, several  
573 regionalization procedures, as for instance summarized in Cislaghi et al. (2020), could be  
574 conveniently applied to transfer model parameters from hydrologically similar catchments to a  
575 catchment of interest. In particular, the regionalization of model parameters could allow to: i) estimate  
576 discharge and runoff time series over ungauged basins overcoming the need of discharge data  
577 recorded from in-situ networks; ii) estimate the model parameter values through a physically  
578 consistent approach, linking them to the characteristics of the basins; iii) solve the problem of  
579 discontinuities in the model parameters, avoiding to obtain patchy unrealistic runoff maps. As this  
580 aspect requires additional investigations and it is beyond the paper purpose, it will not be tackled  
581 here.

582 By looking at technical reviews of large-scale hydrological models (e.g., Sood and Smakhtin, 2015,  
583 Kauffeldt et al., 2016), it can be noted there are many established models, similar in objective and  
584 limitations to STREAM v1.3 model, already existing with support and user base (e.g., among others,  
585 Community Land Model, CLM, Oleson et al., 2013; European Hydrological Predictions for the  
586 Environment, E-HYPE, Lindström et al., 2010; H08, Hanasaki et al., 2008, PCR-GLOBWB, van  
587 Beek and Bierkens, 2008; Water – a Global Assessment and Prognosis WaterGAP, Alcamo et al.,  
588 2003; ParFlow-CLM, Maxwell et al., 2015; WRF-Hydro, Gochis et al., 2018). Some of them, e.g.,  
589 ParFlow-CLM or WRF-Hydro have been specifically configured across the continental United States  
590 and showed good capability to reproduce observed streamflow data over the Mississippi river basin



591 with performances decreased throughout the Great Plains (O'Neill et al., 2020, Tijerina et al., 2021)  
592 which is consistent with the results we obtained with STREAM v1.3 model. However, with respect  
593 to classical hydrological and land surface models, STREAM v1.3 is based on a new concept for  
594 estimating runoff and river discharge which relies on: (a) the almost exclusive use of satellite  
595 observations, and, (b) a simplification of the processes being modelled.  
596 This approach brings several advantages: 1) satellite data implicitly consider the human impact on  
597 the water cycle observing some processes, such as irrigation application or groundwater withdrawals,  
598 that are affected by large uncertainty in classical hydrological models, 2) the satellite technology  
599 grows quickly and hence it is expected that the spatial/temporal resolution and accuracy of satellite  
600 products will be improved in the near future (e.g., 1 km resolution from new satellite soil moisture  
601 products and the next generation gravity mission); the STREAM v1.3 model is able to fully exploit  
602 such improvements; 3) STREAM v1.3 model simulates only the most important processes affecting  
603 the generation of runoff, and considers only the most important variables as input (precipitation,  
604 surface soil moisture and groundwater storage). In other words, the model does not need to simulate  
605 processes, such as evapotranspiration and infiltration and therefore it is an independent modelling  
606 approach for simulating runoff and river discharge that can be also exploited for benchmarking and  
607 improving classical land surface and hydrological models.

## 608 **8. CONCLUSIONS**

609 This study presents a new conceptual hydrological model, STREAM v1.3, for runoff and river  
610 discharge estimation. By using as input satellite data of precipitation, soil moisture and terrestrial  
611 water storage anomalies, the model has been able to provide accurate daily river discharge and runoff  
612 estimates at the outlet river section and the inner river sections and over a  $0.25^{\circ} \times 0.25^{\circ}$  spatial grid of  
613 the Mississippi river basin. In particular, the model is suitable to reproduce:  
614 1. river discharge time series over the calibrated river section with good performances both in  
615 calibration and validation periods;

616 2. river discharge time series over river sections not used for calibration and not located downstream  
617 dams or reservoirs;

618 3. runoff time series with a quite good agreement with respect to the well-established GRUN  
619 observational-based dataset used for comparison.

620 The integration of observations of soil moisture, precipitation and terrestrial water storage anomalies  
621 is a first alternative method for river discharge and runoff estimation with respect to classical methods  
622 based on the use of TWSA-only (suitable for river basins larger than 160'000 km<sup>2</sup>, monthly time  
623 scale) or on classical LSMs (Cai et al., 2014).

624 Moreover, although simple, the model has demonstrated a great potential to be easily applied over  
625 subbasins with different climatic and topographic characteristics, suggesting also the possibility to  
626 extend its application to other basins. In particular, the analysis over basins with high human impact,  
627 where the knowledge of the hydrological cycle and the river discharge monitoring is very important,  
628 deserves special attention. Indeed, as the STREAM v1.3 model is directly ingesting observations of  
629 soil moisture and terrestrial water storage data, it allows the modeller to neglect processes that are  
630 implicitly accounted for in the input data. Therefore, human-driven processes (e.g., irrigation, land  
631 use change), that are typically very difficult to simulate due to missing information and might have a  
632 large impact on the hydrological cycle, hence on total runoff, could be implicitly modelled. The  
633 application of the STREAM v1.3 model on a larger number of basins with different climatic-  
634 physiographic characteristics (e.g., including more arid basins, snow-dominated, lots of topography,  
635 heavily managed) will allow to investigate the possibility to regionalize the model parameters and  
636 overcome the limitations of the automatic calibration procedure highlighted in the discussion section.

## 637 **AUTHOR CONTRIBUTION**

638 S.C. performed the analysis and wrote the manuscript. G.G. collected the data and helped in  
639 performing the analysis; C.M, L.B., A.T., N.S., H.H.F., C.M., M.R. and J.B. contributed to the  
640 supervision of the work. All authors discussed the results and contributed to the final manuscript.

641 **CODE AVAILABILITY**

642 The STREAM model version 1.3, with a short user manual, is freely downloadable in Zenodo  
643 (<https://zenodo.org/record/4744984>, doi: 10.5281/zenodo.4744984). The STREAM v1.3 model code  
644 is distributed through M language files, but it could be run with different interpreters of M language,  
645 like the GNU Octave (freely downloadable here <https://www.gnu.org/software/octave/download>).

646 **DATA AVAILABILITY**

647 All data and codes used in the study are freely available online. Air temperature data are available at  
648 <https://psl.noaa.gov/data/gridded/data.cpc.globaltemp.html> (last access 25/11/202). In situ river  
649 discharge data have been taken from the Global Runoff Data Center (GRDC,  
650 [https://www.bafg.de/GRDC/EN/Home/homepage\\_node.html](https://www.bafg.de/GRDC/EN/Home/homepage_node.html) (last access 25/11/202). Precipitation  
651 and soil moisture data are available from <http://pmm.nasa.gov/data-access/downloads/trmm> and  
652 <https://esa-soilmoisture-cci.org/>, respectively.

653 **COMPETING INTERESTS**

654 The authors declare that they have no conflict of interest.

655 **ACKNOWLEDGMENTS**

656 The authors wish to thank the Global Runoff Data Centre (GRDC) for providing most of the  
657 streamflow data throughout Europe. The authors gratefully acknowledge support from ESA through  
658 the STREAM Project (EO Science for Society element Permanent Open Call contract n°  
659 4000126745/19/I-NB).

660

## 661 REFERENCE

- 662 Albergel, C., Rüdiger, C., Carrer, D., Calvet, J. C., Fritz, N., Naeimi, V., Batalis, Z., and Hasenauer, S.: An evaluation  
663 of ASCAT surface soil moisture products with in-situ observations in southwestern France, *Hydrol. Earth Syst. Sci.*,  
664 13, 115–124, <https://doi.org/doi:10.5194/hess-13-115-2009>, 2009.
- 665 Alcamo, J., Döll, P., Henrichs, T., Kaspar, F., Lehner, B., Rösch, T., & Siebert, S.: Development and testing of the  
666 WaterGAP 2 global model of water use and availability, *Hydrol. Sci. J.*, 48(3), 317-337,  
667 <https://doi.org/10.1623/hysj.48.3.317.45290>, 2003.
- 668 Alexander, J. S., Wilson, R. C., and Green, W. R.: A brief history and summary of the effects of river engineering and  
669 dams on the Mississippi River system and delta (p. 53), US Department of the Interior, US Geological Survey,  
670 <https://doi.org/10.3133/cir1375>, 2012.
- 671 Allen, R.G., Pereira, L. S., Raes, D., and Smith, M.: Crop evapotranspiration — guidelines for computing crop water  
672 requirements. FAO Irrigation & Drainage Paper 56. FAO, Rome, 1988.
- 673 Arabzadeh, A., and Behrangi, A.: Investigating Various Products of IMERG for Precipitation Retrieval Over Surfaces  
674 With and Without Snow and Ice Cover, *Remote Sens.*, 13(14), 2726; <https://doi.org/10.3390/rs13142726>, 2021.
- 675 Balsamo, G., A. Beljaars, K. Scipal, P. Viterbo, B. vanden Hurk, M. Hirschi, and A. K. Betts: A revised hydrology for  
676 the ECMWF model: Verification from field site to terrestrial water storage and impact in the integrated forecast  
677 system, *J. Hydrometeorol.*, 10(3), 623–643, <https://doi.org/doi:10.1175/2008JHM1068.1>, 2009.
- 678 Barbarossa, V., Huijbregts, M. A., Beusen, A. H., Beck, H. E., King, H., and Schipper, A. M.: FLO1K, global maps of  
679 mean, maximum and minimum annual streamflow at 1 km resolution from 1960 through 2015, *Scientific Sci. Data*,  
680 5, 180052, <https://doi.org/10.1038/sdata.2018.52>, 2018.
- 681 Beck, H. E., van Dijk, A. I., de Roo, A., Dutra, E., Fink, G., Orth, R., and Schellekens, J.: Global evaluation of runoff  
682 from ten state-of-the-art hydrological models, *Hydrol. Earth Syst. Sci.*, 21(6), 2881-2903. <https://doi.org/doi:10.5194/hess-21-2881-2017>, 2017.
- 684 Berghuijs, W. R., Woods, R. A., Hutton, C. J., and Sivapalan, M.: Dominant flood generating mechanisms across the  
685 United States, *Geophys. Res. Lett.*, 43, 4382–4390, <https://doi.org/10.1002/2016GL068070>, 2016.
- 686 Berthet, L., Andréassian, V., Perrin, C., and Javelle, P.: How crucial is it to account for the antecedent moisture conditions  
687 in flood forecasting? Comparison of event-based and continuous approaches on 178 catchments, *Hydrol. Earth Syst.*  
688 *Sci.*, 13(6), 819-831, 2009.
- 689 Blöschl, G., Sivapalan, M., Wagener, T., Viglione, A., and Savenije, H. H. G. (Eds.): *Runoff predictions in ungauged*  
690 *basins: A synthesis across processes, places and scales*, Cambridge: Cambridge University Press, 2013.
- 691 Bober, W. *Introduction to Numerical and Analytical Methods with MATLAB for Engineers and Scientists*; CRC Press,  
692 Inc.: Boca Raton, FL, USA, <https://doi.org/10.1201/b16030>, 2013.
- 693 Botter, G., Porporato, A., Daly, E., Rodriguez-Iturbe, I., and Rinaldo, A.: Probabilistic characterization of base flows in  
694 river basins: Roles of soil, vegetation, and geomorphology, *Water Resour. Res.*, 43, W06404,  
695 <https://doi.org/doi:10.1029/2006WR005397>, 2007a.
- 696 Botter, G., Peratoner, F., Porporato, A., Rodriguez-Iturbe, I., and Rinaldo, A.: Signatures of large-scale soil moisture  
697 dynamics on streamflow statistics across U.S. Climate regimes, *Water Resour. Res.*, 43, W11413,  
698 <https://doi.org/doi:10.1029/2007WR006162>, 2007b.
- 699 Brocca, L., Melone, F., and Moramarco, T.: On the estimation of antecedent wetness conditions in rainfall-runoff  
700 modelling, *Hydrol. Process.*, 22 (5), 629-642, doi:10.1002/hyp.6629. <https://doi.org/10.1002/hyp.6629>, 2008.
- 701 Brocca, L., Melone, F., Moramarco, T., and Morbidelli, R.: Antecedent wetness conditions based on ERS scatterometer  
702 data, *J. Hydrol.*, 364(1-2), 73-87, <https://doi.org/10.1016/j.jhydrol.2008.10.007>, 2009.
- 703 Brocca, L., Melone, F., and Moramarco, T.: Distributed rainfall-runoff modelling for flood frequency estimation and  
704 flood forecasting, *Hydrol. Process.*, 25(18), 2801-2813, <https://doi.org/10.1002/hyp.8042>, 2011.

705 Brocca, L., Ciabatta, L., Massari, C., Camici, S., and Tarpanelli, A.: Soil moisture for hydrological applications: open  
706 questions and new opportunities, *Water*, 9(2), 140, <https://doi.org/10.3390/w9020140>, 2017.

707 Cai, X., Yang, Z. L., David, C. H., Niu, G. Y., and Rodell, M.: Hydrological evaluation of the Noah-MP land surface  
708 model for the Mississippi River Basin, *J. Geophys. Res. Atmos.*, 119(1), 23-38,  
709 <https://doi.org/10.1002/2013JD020792>, 2014.

710 Cislighi, A., Masseroni, D., Massari, C., Camici, S., and Brocca, L.: Combining a rainfall-runoff model and a  
711 regionalization approach for flood and water resource assessment in the western Po Valley, Italy, *Hydrol. Sci. J.*,  
712 65(3), 348-370, <https://doi.org/10.1080/02626667.2019.1690656>, 2020.

713 Crochemore, L., Isberg, K., Pimentel, R., Pineda, L., Hasan, A., and Arheimer, B.: Lessons learnt from checking the  
714 quality of openly accessible river flow data worldwide, *Hydrol. Sci. J.*, 65(5), 699-711,  
715 <https://doi.org/10.1080/02626667.2019.1659509>, 2020.

716 Crow, W. T., Bindlish, R., and Jackson, T. J.: The added value of spaceborne passive microwave soil moisture retrievals  
717 for forecasting rainfall-runoff partitioning, *Geophys. Res. Lett.*, 32(18), <https://doi.org/10.1029/2005GL023543>,  
718 2005.

719 Döll, P., F.Kaspar, and B.Lehner: A global hydrological model for deriving water availability indicators: Model tuning  
720 and validation, *J. Hydrol.*, 270(1-2), 105-134, [https://doi.org/doi:10.1016/S0022-1694\(02\)00283-4](https://doi.org/doi:10.1016/S0022-1694(02)00283-4), 2003.

721 Dorigo, W., Wagner, W., Albergel, C., Albrecht, F., Balsamo, G., Brocca, L., Chung, D., Ertl, M., Forkel, M., Gruber, A.,  
722 Haas, D., Hamer, P., Hirschi, M., Ikonen, J., de Jeu, R., Kidd, R., Lahoz, W., Liu, Y.Y., Miralles, D., Mistelbauer, T.,  
723 Nicolai-Shaw, N., Parinussa, R., Pratola, C., Reimer, C., van der Schalie, R., Seneviratne, S.I., Smolander, T., and  
724 Lecomte, P.: ESA CCI Soil Moisture for improved Earth system understanding: state-of-the art and future directions.,  
725 *Remote Sens. Environ.*, 203, 185-215, <https://doi.org/10.1016/j.rse.2017.07.001>, 2017.

726 Dyer, J.: Snow depth and streamflow relationships in large North American watersheds, *J. Geophys. Res.*, 113, D18113,  
727 <https://doi.org/10.1029/2008JD010031>, 2008.

728 Entekhabi, D., Njoku, E. G., O'Neill, P. E., Kellogg, K. H., Crow, W. T., Edelstein, W. N., ... and Van Zyl, J.: The soil  
729 moisture active passive (SMAP) mission. *Proceedings of the Institute of Electrical and Electronics Engineers (IEEE)*,  
730 98(5), 704-716. <https://doi.org/doi:10.1109/JPROC.2010.2043918>, 2010.

731 Famiglietti, J.S., and Wood, E. F.: Multiscale modeling of spatially variable water and energy balance processes, *Water*  
732 *Resour. Res.*, 30, 3061-3078, <https://doi.org/10.1029/94WR01498>, 1994.

733 Famiglietti, J. S., and Rodell, M.: Water in the balance, *Science*, 340(6138), 1300-1301,  
734 <https://doi.org/10.1126/science.1236460>, 2013.

735 Fan, Y. and Van den Dool, H. A: Global monthly land surface air temperature analysis for 1948-present, *J. Geophys.*  
736 *Res. Atmos.*, 113, D01103, <https://doi.org/10.1029/2007JD008470>, 2008.

737 Fekete, B. M., Looser, U., Pietroniro, A., and Robarts, R. D.: Rationale for monitoring discharge on the ground, *J.*  
738 *Hydrometeorol.*, 13, 1977-1986, <https://doi.org/10.1175/JHM-D-11-0126.1>, 2012.

739 Georgakakos KP, and Baumer OW.: Measurement and utilization of onsite soil moisture data, *J. Hydrol.*, 184: , 131-152,  
740 [https://doi.org/10.1016/0022-1694\(95\)02971-0](https://doi.org/10.1016/0022-1694(95)02971-0), 1996.

741 Ghiggi, G., Humphrey, V., Seneviratne, S. I., and Gudmundsson, L.: GRUN: an observation-based global gridded runoff  
742 dataset from 1902 to 2014, *Earth Syst. Sci. Data*, 11, 1655-1674 *Earth System Science Data*, 11(4), 1655-1674,  
743 <https://doi.org/10.5194/essd-11-1655-2019>, 2019.

744 Ghotbi, S., Wang, D., Singh, A., Blöschl, G., and Sivapalan, M.: A New Framework for Exploring Process Controls of  
745 Flow Duration Curves, *Water Resour. Res. Water Resources Research*, 56(1), <https://doi.org/e2019WR026083>, 2020.

746 Gochis, D. J., Barlage, M., Dugger, A., FitzGerald, K., Karsten, L., McAllister, M., et al. (2018). The WRF-Hydro  
747 modeling system technical description, (Version 5.0). NCAR Technical Note. Retrieved from  
748 <https://ral.ucar.edu/sites/default/files/public/WRFHydroV5TechnicalDescription.pdf>

749 Gudmundsson, L., Wagener, T., Tallaksen, L. M., and Engeland, K.: Evaluation of nine large-scale hydrological models  
750 with respect to the seasonal runoff climatology in Europe, *Water Resour. Res.*, 48(11),  
751 <https://doi.org/10.1029/2011WR010911>, 2012a.

752 Gudmundsson, L., Tallaksen, L. M., Stahl, K., Clark, D. B., Du-mont, E., Hagemann, S., Bertrand, N., Gerten, D., Heinke,  
753 J., Hanasaki, N., Voss, F., and Koirala, S.: Comparing Large-Scale Hydrological Model Simulations to Observed  
754 Runoff Percentiles in Europe, *J. Hydrometeorol.*, 13, 604–62, <https://doi.org/10.1175/JHM-D-11-083.1>, 2012b.

755 Gudmundsson, L., and Seneviratne, S. I.: Observation-based gridded runoff estimates for Europe (E-RUN version 1.1),  
756 *Earth Syst. Sci. Data*, 8, 279–295, <https://doi.org/10.5194/essd-8-279-2016>, 8(2), 279-295 2016, 2016.

757 Gupta VK, Waymire E, and Wang CT.: A representation of an instantaneous unit hydrograph from geomorphology, *Water*  
758 *Resour. Res.*, 16: 855–862, <https://doi.org/doi:10.1029/WR016i005p00855>, 1980.

759 Gupta, H. V., Kling, H., Yilmaz, K. K., and Martinez, G. F.: Decomposition of the mean squared error and NSE  
760 performance criteria: Implications for improving hydrological modelling, *J. Hydrol.*, 377(1-2), 80-91,  
761 <https://doi.org/10.1016/j.jhydrol.2009.08.003>, 2009.

762 Haddeland, I., Heinke, J., Voß, F., Eisner, S., Chen, C., Hagemann, S., and Ludwig, F.: Effects of climate model radiation,  
763 humidity and wind estimates on hydrological simulations, *Hydrol. Earth Syst. Sci.*, 16(2), 305-318,  
764 <https://doi.org/10.5194/hess-16-305-2012>, 2012.

765 Hanasaki, N., Kanae, S., Oki, T., Masuda, K., Motoya, K., Shirakawa, N., ... , and Tanaka, K. :An integrated model for  
766 the assessment of global water resources–Part 1: Model description and input meteorological forcing, *Hydrol. Earth*  
767 *Syst. Sci.*, 12(4), 1007-1025, <https://doi.org/10.5194/hess-12-1007-2008>, 2008.

768 Hastie, T., Tibshirani, R., and Friedman, J. H.: The Elements of Statistical Learning – Data Mining, Inference, and  
769 Prediction, Second Edition, Springer Series in Statistics, Springer, New York, 2nd Edn., available at: [http://www-](http://www-stat.stanford.edu/~tibs/ElemStatLearn/)  
770 [stat.stanford.edu/~tibs/ElemStatLearn/](http://www-stat.stanford.edu/~tibs/ElemStatLearn/) (last access: 5 July 2016)., 2009.

771 Hong, Y., Adler, R. F., Hossain, F., Curtis, S., and Huffman, G. J.: A first approach to global runoff simulation using  
772 satellite rainfall estimation, *Water Resour. Res.*, 43(8), <https://doi.org/10.1029/2006WR005739>, 2007.

773 Horton, R. E.: Hydrological approach to quantitative morphology, *Geol. Soc. Am. Bull.*, 56, 275-370, 1945.

774 Houborg, R., Rodell, M., Li, B., Reichle, R., and Zaitchik, B. F.: Drought indicators based on model-assimilated Gravity  
775 Recovery and Climate Experiment (GRACE) terrestrial water storage observations, *Water Resour. Res.*, 48(7),  
776 <https://doi.org/10.1029/2011WR011291>, 2012.

777 Hu GR., and Li XY.: Subsurface Flow. In: Li X., Vereecken H. (eds) Observation and Measurement. Ecohydrology.  
778 Springer, Berlin, Heidelberg. [https://doi.org/10.1007/978-3-662-47871-4\\_9-1](https://doi.org/10.1007/978-3-662-47871-4_9-1), 2018.

779 Huffman, G. J., Adler, R. F., Bolvin, D. T., Gu, G. J., Nelkin, E. J., Bowman, K. P., Hong, Y., Stocker, E. F. and Wolff,  
780 D. B.: The TRMM Multisatellite Precipitation Analysis (TMPA): Quasi-Global, Multiyear, Combined-Sensor  
781 Precipitation Estimates at Fine Scales, *J. Hydrometeorol.*, 8 (1): 38–55. <https://doi.org/doi:10.1175/jhm560.1>, 2007.

782 Huffman, G. J., Stocker, E. F., Bolvin, D. T., Nelkin, E. J., and Adler, R. F.: TRMM Version 7 3B42 and 3B43 Data Sets.  
783 NASA/GSFC, Greenbelt, MD, 2014.

784 Huffman, G. J., Bolvin, D. T., Braithwaite D., Hsu K., Joyce R. , Kidd C., Nelkin Eric J., Sorooshian S., Tan J., and Xie  
785 P.: NASA Global Precipitation Measurement (GPM) Integrated Multi-satellitE Retrievals for GPM (IMERG),.  
786 [https://docsserver.gesdisc.eosdis.nasa.gov/public/project/GPM/IMERG\\_ATBD\\_V06.pdf](https://docsserver.gesdisc.eosdis.nasa.gov/public/project/GPM/IMERG_ATBD_V06.pdf), 2019.

787 Kauffeldt, A., Wetterhall, F., Pappenberger, F., Salamon, P., & Thielen, J.: Technical review of large-scale hydrological  
788 models for implementation in operational flood forecasting schemes on continental level, *Environ. Model. Softw.*, 75,  
789 68-76, <https://doi.org/10.1016/j.envsoft.2015.09.009>, 2016.

790 Kim, H., Watanabe, S., Chang, E. C., Yoshimura, K., Hirabayashi, J., Famiglietti, J., and Oki, T.: Global Soil Wetness  
791 Project Phase 3 Atmospheric Boundary Conditions (Experiment 1) [Data set], Data Integration and Analysis System  
792 (DIAS), <https://doi.org/10.20783/DIAS.501>, 2017.

793 Kirchner, J. W.: Getting the right answers for the right reasons: Linking measurements, analyses, and models to advance  
794 the science of hydrology, *Water Resour. Res.*, 42(3), <https://doi.org/10.1029/2005WR004362>, 2006.

795 Klees, R., Revtova, E. A., Gunter, B.C. , Ditmar, P., Oudman, E., Winsemius H. C., and Savenije H.H.G.: The design of  
796 an optimal filter for monthly GRACE gravity models, *Geoph. J. Intern.*, 175 (2): 417–432,  
797 <https://doi.org/10.1111/j.1365-246X.2008.03922.x>, 2008

798 Kling, H., Fuchs, M., and Paulin, M.: Runoff conditions in the upper Danube basin under an ensemble of climate change  
799 scenarios, *J. Hydrol.*, 424, 264-277, <https://doi.org/doi:10.1016/j.jhydrol.2012.01.011>, 2012.

800 Landerer, F. W., and Swenson, S. C.: Accuracy of scaled GRACE terrestrial water storage estimates, *Water Resour. Res.*,  
801 48(4), <https://doi.org/10.1029/2011WR011453>, 2012.

802 Lehner, B., C. Reidy Liermann, C. Revenga, C. Vörösmarty, B. Fekete, P. Crouzet, P. Döll, M. Endejan, K. Frenken, J.  
803 Magome, C. Nilsson, J.C. Robertson, R. Rodel, N. Sindorf, and D. Wisser.: High-resolution mapping of the world's  
804 reservoirs and dams for sustainable river-flow management, *Front. Ecol. Environ.*, 9 (9),: 494-502,  
805 <https://doi.org/10.1890/100125>, 2011.

806 Lindström, G., Pers, C., Rosberg, J., Strömquist, J., & Arheimer, B.: Development and testing of the HYPE (Hydrological  
807 Predictions for the Environment) water quality model for different spatial scales, *Hydrol. Res.*, 41(3-4), 295-319,  
808 <https://doi.org/10.2166/nh.2010.007>, 2010.

809 Long, D., Longuevergne, L., and Scanlon, B. R.: Uncertainty in evapotranspiration from land surface modeling, remote  
810 sensing, and GRACE satellites, *Water Resour. Res.*, 50(2), 1131-1151, <https://doi.org/10.1002/2013WR014581>,  
811 2014.

812 Lorenz, C., H. Kunstmann, H., B. Devaraju, B., Tourian, M. J., N. Sneeuw, N., and J. Riegger, J.: Large-Scale Runoff  
813 from Landmasses: A Global Assessment of the Closure of the Hydrological and Atmospheric Water Balances., *J.*  
814 *Hydrometeor.*, 15, 2111–2139, <https://doi.org/doi:10.1175/JHM-D-13-0157.1>, 2014.

815 Luthcke, S.B., Sabaka, T.J., Loomis, B.D., Arendt, A.A., McCarthy, J.J., and Camp, J.: Antarctica, Greenland and Gulf  
816 of Alaska land-ice evolution from an iterated GRACE global mascon solution, *J. Glaciol.*, Vol. 59, No. 216, 613-631,  
817 2013 <https://doi.org/doi:10.3189/2013JoG12J147>, 2013.

818 Massari, C., Brocca, L., Barbetta, S., Papathanasiou, C., Mimikou, M., and Moramarco, T.: Using globally available soil  
819 moisture indicators for flood modelling in Mediterranean catchments, *Hydrol. Earth Syst. Sci.*, 18(2), 839,  
820 <https://doi.org/10.5194/hess-18-839-2014>, 2014.

821 Massari, C., Brocca, L., Tarpanelli, A., Hong, Y., Crow, W., Ciabatta, L., Camici, S., Barbetta, S., and Moramarco, T.:  
822 Global surface runoff estimation in near real time by using SMAP and GPM, poster at SMAP conference, 2016.

823 Maxwell, R. M., Condon, L. E., and Kollet, S. J.: A high-resolution simulation of groundwater and surface water over  
824 most of the continental US with the integrated hydrologic model ParFlow v3, *Geosci. Model Dev.*, 8, 923–937,  
825 <https://doi.org/10.5194/gmd-8-923-2015>, 2015.

826 Merz, R., and and Blöschl, G.: A regional analysis of event runoff coefficients with respect to climate and catchment  
827 characteristics in Austria, *Water Resour. Res.*, 45(1), <https://doi.org/10.1029/2008WR007163>, 2009.

828 Mueller Schmied, H., Adam, L., Eisner, S., Fink, G., Flörke, M., Kim, H., ... and Song, Q.: Variations of global and  
829 continental water balance components as impacted by climate forcing uncertainty and human water use, *Hydrol. Earth*  
830 *Syst. Sci.*, 20(7), 2877-2898, <https://doi.org/10.5194/hess-20-2877-2016>, 2016.

831 Muneeppeerakul, R., Azaele, S., Botter, G., Rinaldo, A., and Rodriguez-Iturbe, I.: Daily streamflow analysis based on a  
832 two-scaled gamma pulse model, *Water Resour. Res.*, 46(11), <https://doi.org/10.1029/2010WR009286>, 2010.

833 Nash, J. E.: The form of the instantaneous unit hydrograph, *IASH publication no. 45*, 3–4, 114–121, 1957.

834 Natural Resources Conservation Service (NRCS): Urban hydrology for small watersheds, Tech. Release 55, 2nd ed., U.S.  
835 Dep. of Agric., Washington, D. C. (available at [ftp://ftp.wcc.nrcs.usda.gov/downloads/](ftp://ftp.wcc.nrcs.usda.gov/downloads/hydrology_hydraulics/tr55/tr55.pdf)  
836 [hydrology\\_hydraulics/tr55/tr55.pdf](ftp://ftp.wcc.nrcs.usda.gov/downloads/hydrology_hydraulics/tr55/tr55.pdf)), 1986.

837 Oleson, K., Lawrence, D. M., Bonan, G. B., Drewniak, B., Huang, M., Koven, C. D., ... Yang, Z. -L.: Technical  
838 description of version 4.5 of the Community Land Model (CLM) (No. NCAR/TN-503+STR).  
839 <http://dx.doi.org/10.5065/D6RR1W7M>, 2013.

840 Orth, R., and Seneviratne, S. I.: Introduction of a simple-model-based land surface dataset for Europe, *Environ. Res. Lett.*,  
841 10(4), 044012, <https://doi.org/10.1088/1748-9326/10/4/044012>, 2015.

842 Pellet, V., Aires, F., Munier, S., Fernández Prieto, D., Jordá, G., Dorigo, W. A., ... and Brocca, L.: Integrating multiple  
843 satellite observations into a coherent dataset to monitor the full water cycle—application to the Mediterranean region.,  
844 *Hydrol. Earth Syst. Sci.*, 23(1), 465-491, <https://doi.org/10.5194/hess-23-465-2019>, 2019.



845 Prudhomme, C., Giuntoli, I., Robinson, E. L., Clark, D. B., Arnell, N. W., Dankers, R., ... and Hagemann, S.: Hydrological  
846 droughts in the 21st century, hotspots and uncertainties from a global multimodel ensemble experiment, *Proceedings*  
847 *of the National Academy of Sciences*, 111(9), 3262-3267, 2014.

848 Rakovec, O., Kumar, R., Attinger, S., and Samaniego, L.: Improving the realism of hydrologic model functioning through  
849 multivariate parameter estimation, *Water Resour. Res.*, 52(10), 7779-7792, <https://doi.org/10.1002/2016WR019430>,  
850 2016.

851 Richards, L.A.: Capillary conduction of liquids through porous mediums, *Physics*. 1 (5): 318-333.,  
852 Bibcode:1931Physi.1.318R., <https://doi.org/doi:10.1063/1.1745010>, 1931.

853 Riegger, J., and Tourian, M. J.: Characterization of runoff-storage relationships by satellite gravimetry and remote  
854 sensing, *Water Resour. Res.*, 50, 3444-3466, <https://doi.org/doi:10.1002/2013WR013847>, 2014.

855 Rodell, M., Beaudoin, H. K., L'Ecuyer, T. S., Olson, W. S., Famiglietti, J. S., Houser, P. R., Adler, R., Bosilovich, M.  
856 G., Clayson, C. A., Chambers, D., Clark, E., Fetzer, E. J., Gao, X., Gu, G., Hilburn, K., Huffman, G. J., Lettenmaier,  
857 D. P., Liu, W. T., Robertson, F. R., Schlosser, C. A., Sheffield, J. and Wood, E. F.: The observed state of the water  
858 cycle in the early 15twenty-first century, *J. Clim.*, 28(21), 8289-8318, [https://doi.org/doi:10.1175/JCLI-D-14-](https://doi.org/doi:10.1175/JCLI-D-14-00555.1)  
859 [00555.1](https://doi.org/doi:10.1175/JCLI-D-14-00555.1), 2015.

860 Schellekens, J., Dutra, E., Martínez-de la Torre, A., Balsamo, G., van Dijk, A., Sperna Weiland, F., Minvielle, M., Cal-  
861 vet, J.-C., Decharme, B., Eisner, S., Fink, G., Flörke, M., Peßenteiner, S., van Beek, R., Polcher, J., Beck, H., Orth, R.,  
862 Calton, B., Burke, S., Dorigo, W., and Weedon, G. P.: A global water resources ensemble of hydrological models: the  
863 earthH2Observe Tier-1 dataset, *Earth Syst. Sci. Data*, 9, 389-413, <https://doi.org/10.5194/essd-9-389-2017>, 2017.

864 Schwanghart, W., and Kuhn, N. J.: TopoToolbox: A set of Matlab functions for topographic analysis., *Environ. Model.*  
865 *Softw. Environmental Modelling & Software*, 25(6), 770-781, 2010.

866 Seneviratne, S. I., Corti, T., Davin, E. L., Hirschi, M., Jaeger, E. B., Lehner, I., ... and Teuling, A. J.: Investigating soil  
867 moisture-climate interactions in a changing climate: A review, *Earth-Sci. Rev.*, 99(3-4), 125-161,  
868 <https://doi.org/10.1016/j.earscirev.2010.02.004>, 2010.

869 Sneeuw, N., Lorenz, C., Devaraju, B., Tourian, M. J., Riegger, J., Kunstmann, H., and Bárdossy, A.: Estimating runoff  
870 using hydro-geodetic approaches, *Surv. Geophys.*, 35(6), 1333-1359, <https://doi.org/10.1007/s10712-014-9300-4>,  
871 2014.

872 Solomatine, D. P., and Ostfeld, A.: Data-driven modelling: some past experiences and new approaches, *J. Hydroinform.*,  
873 10(1), 3-22, <https://doi.org/10.2166/hydro.2008.015>, 2008.

874 Sood, A., and Smakhtin, V.: Global hydrological models: a review, *Hydrol. Sci. J.*, 60(4), 549-565,  
875 <https://doi.org/10.1080/02626667.2014.950580>, 2015.

876 Strahler, A. N.: Hypsometric (area-altitude) analysis of erosional topography, *Geol. Soc. Am. Bull. Geological Society of*  
877 *America Bulletin*, 63(11), 1117-1142, [https://doi.org/10.1130/0016-7606\(1952\)63\[1117:HAAOET\]2.0.CO;2](https://doi.org/10.1130/0016-7606(1952)63[1117:HAAOET]2.0.CO;2), 1952.

878 Tapley, B.D., Watkins, M.M., Flechtner, F. et al.: Contributions of GRACE to understanding climate change, *Nat. Clim.*  
879 *Chang.*, 9, 358-369, <https://doi.org/doi:10.1038/s41558-019-0456-2>, 2019.

880 Thiémié, V., Rojas, R., Zambrano-Bigiarini, M., and De Roo, A.: Hydrological evaluation of satellite rainfall estimates  
881 over the Volta and Baro-Akobo Basin, *J. Hydrol.*, 499, 324-338, <https://doi.org/10.1016/j.jhydrol.2013.07.012>, 2013.

882 Tourian, M. J., Reager, J. T., and Sneeuw, N.: The total drainable water storage of the Amazon river basin: A first estimate  
883 using GRACE, *Water Resour. Res.*, 54., <https://doi.org/10.1029/2017WR021674>, 2018.

884 Trambly, Y., Bouvier, C., Martin, C., Didon-Lescot, J. F., Todorovik, D., and Domergue, J. M.: Assessment of initial  
885 soil moisture conditions for event-based rainfall-runoff modelling, *J. Hydrol.*, 387(3-4), 176-187,  
886 <https://doi.org/10.1016/j.jhydrol.2010.04.006>, 2010.

887 Troutman, B. M., and Karlinger, M.B.: Unit hydrograph approximation assuming linear flow through topologically  
888 random channel networks, *Water Resour. Res.*, 21., 743 - 754, <https://doi.org/doi:10.1029/WR021i005p00743>, 1985.

889 Van Beek, L. P. H., and Bierkens, M. F. P.: The global hydrological model PCR-GLOBWB: conceptualization,  
890 parameterization and verification. Utrecht University, Utrecht, The Netherlands, 1, 25-26, 2009.



891 Vörösmarty C. J., and Coauthors: Global water data: A newly endangered species, *Eos, Trans. Amer. Geophys. Union*,  
892 82, 54, <https://doi.org/10.1029/01EO00031>, 2002.

893 Vose, R.S., Applequist, S., Durre, I., Menne, M.J., Williams, C.N., Fenimore, C., Gleason, K., and Arndt, D.: Improved  
894 Historical Temperature and Precipitation on Time Series For U.S. Climate Divisions., *J. Meteorol. and Climat.*,  
895 53(May), 1232–1251., <https://doi.org/10.1175/JAMC-D-13-0248.1>DOI: 10.1175/JAMC-D-13-0248.1, 2014.

896 Wagner, W., Lemoine, G., and Rott, H.: A method for estimating soil moisture from ERS scatterometer and soil data.,  
897 *Remote Sens. Environ. Remote Sensing of Environment*, 70, 191–207, [https://doi.org/doi:10.1016/S0034-](https://doi.org/doi:10.1016/S0034-4257(99)00036-X)  
898 [4257\(99\)00036-X](https://doi.org/doi:10.1016/S0034-4257(99)00036-X), 1999.

899 Wagner, W., Blöschl, G., Pampaloni, P., Calvet, J. C., Bizzarri, B., Wigneron, J. P., and Kerr, Y.: Operational readiness  
900 of microwave remote sensing of soil moisture for hydrologic applications, *Hydrol. Res.*, 38(1), 1-20,  
901 <https://doi.org/10.2166/nh.2007.029>, 2007.

902 Wang, Y. H., Broxton, P., Fang, Y., Behrangi, A., Barlage, M., Zeng, X., and Niu, G. Y.: A wet-bulb temperature-based  
903 rain-snow partitioning scheme improves snowpack prediction over the drier western United States, *Geophys. Res.*  
904 *Lett.*, 46(23), 13825-13835, <https://doi.org/10.1029/2019GL085722>, 2019.

905 Wisser, D., Fekete, B. M., Vörösmarty, C. J., and Schumann, A. H.: Reconstructing 20th century global hydrography: a  
906 contribution to the Global Terrestrial Network- Hydrology (GTN-H), *Hydrol. Earth Syst. Sci.*, 14, 1–24,  
907 <https://doi.org/doi:10.5194/hess-14-1-2010>, 2010.

908 Yokoo, Y., and Sivapalan, M.: Towards reconstruction of the flow duration curve: Development of a conceptual  
909 framework with a physical basis, *Hydrol. Earth Syst. Sci.*, 15(9), 2805–2819, [https://doi.org/10.5194/hess-15-2805-](https://doi.org/10.5194/hess-15-2805-2011)  
910 2011, 2011.

911 Zhang, Y., Pan, M., Sheffield, J., Siemann, A. L., Fisher, C. K., Liang, M., ... and Zhou, T.: A Climate Data Record  
912 (CDR) for the global terrestrial water budget: 1984–2010, *Hydrol. Earth Syst. Sci.*, 22, 241–263,  
913 [https://doi.org/10.5194/hess-22-241-2018\(Online\)](https://doi.org/10.5194/hess-22-241-2018(Online)), 22(PNNL-SA-129750), 2018.

915 Table 1. Location of gauging stations over the Mississippi basins and upstream contributing area.  
 916 Bold text is used to indicate stations where the STREAM v1.3 model has been calibrated.

#	River	Station name	Latitude (°)	Longitude (°)	Upstream area (km <sup>2</sup> )	Mean annual river discharge (m <sup>3</sup> /s)	Presence of dam
1	Missouri	Bismarck, ND	-100.82	46.81	481'232	633	Garrison dam
2	Missouri	Omaha, NE	-95.92	41.26	814'371	914	Gavins Point Dam
3	Missouri	Kansas City, MO	-94.59	39.11	1'229'427	1499	---
4	<b>Missouri</b>	<b>Hermann, MO</b>	<b>-91.44</b>	<b>38.71</b>	<b>1'330'000</b>	<b>2326</b>	---
5	Kansas	Wamego, KS	-96.30	39.20	143'054	141	Kanopolis
6	<b>Mississippi</b>	<b>Keokuk, IA</b>	<b>-91.37</b>	<b>40.39</b>	<b>282'559</b>	<b>1948</b>	---
7	Rock	Near Joslin, IL	-90.18	41.56	23'835	199	---
8	Mississippi	Chester, IL	-89.84	37.90	1'776'221	6018	---
9	Arkansas	<b>Murray Dam Near Little Rock, AR</b>	<b>-92.36</b>	<b>34.79</b>	<b>408'068</b>	<b>1249</b>	---
10	<b>Mississippi</b>	<b>Vicksburg, MS</b>	<b>-90.91</b>	<b>32.32</b>	<b>2'866'590</b>	<b>17487</b>	---
11	<b>Ohio</b>	<b>Metropolis, ILL.</b>	<b>-88.74</b>	<b>37.15</b>	<b>496'134</b>	<b>7931</b>	---

917  
 918

919 Table 2. Performance scores obtained over the Mississippi river sections during the calibration and  
920 validation periods.

#	CALIBRATION PERIOD			VALIDATION PERIOD		
SCORE	KGE (-)	R (-)	RRMSE (%)	KGE (-)	R (-)	RRMSE (%)
CALIBRATED SECTIONS						
10	0.78	0.78	30	0.74	0.80	38
9	0.62	0.75	71	0.67	0.85	77
6	0.83	0.84	39	0.73	0.84	46
4	0.77	0.78	46	0.72	0.75	50
11	0.82	0.82	44	0.70	0.86	51
SECTIONS NOT USED FOR CALIBRATION						
1	-3.26	0.08	137	0.20	0.44	96
2	-0.57	0.48	118	0.40	0.53	89
3	0.16	0.71	83	0.39	0.70	72
5	-1.49	0.24	368	-1.26	0.31	358
7	0.53	0.68	71	0.20	0.70	81
8	0.80	0.84	36	0.77	0.84	39

921

922

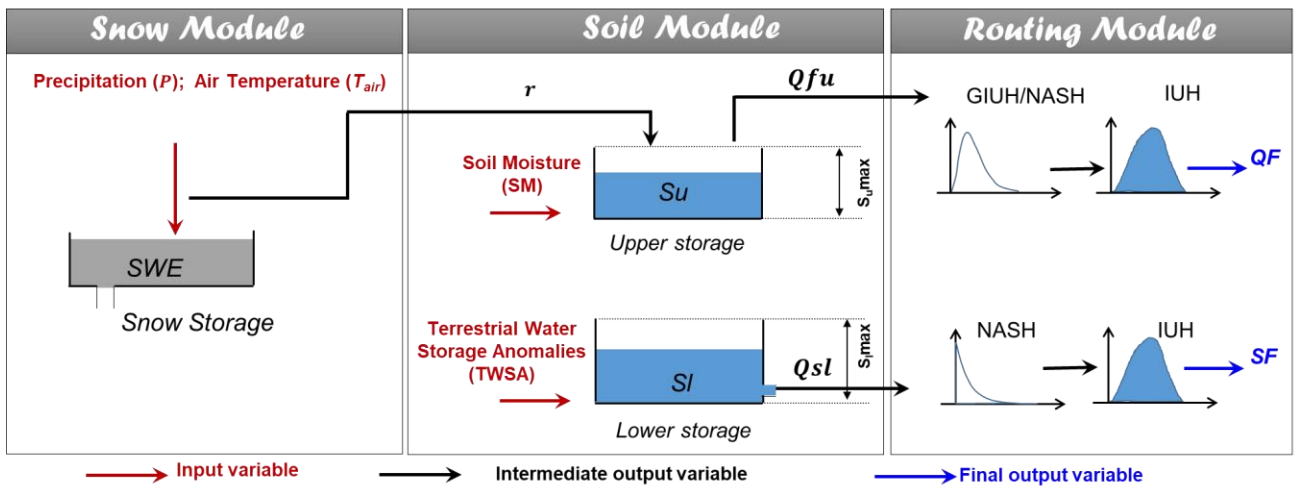
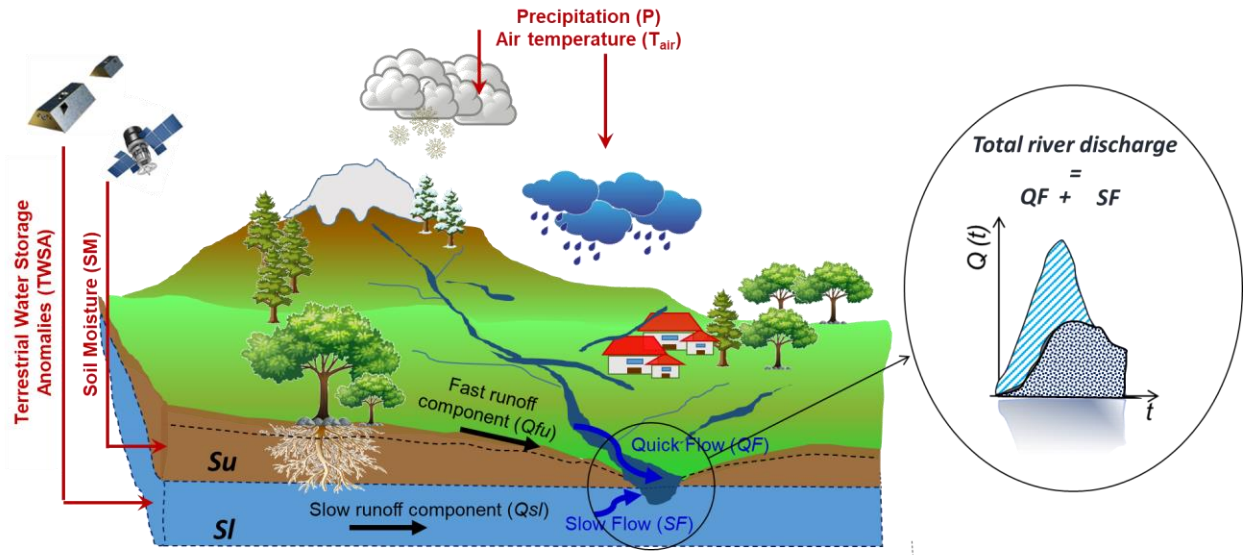
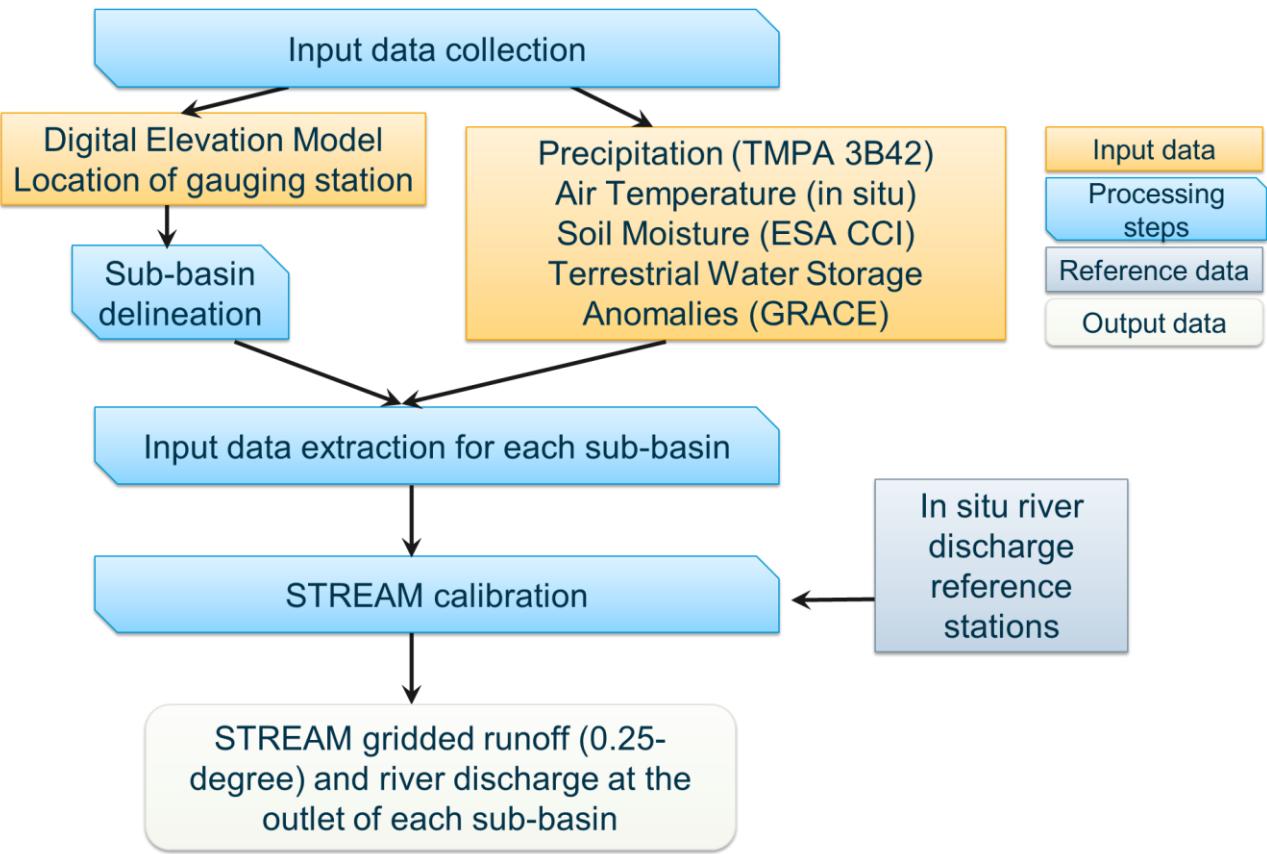


Figure 1. Configuration of the STREAM v1.3 model adopted for total runoff estimation. The model includes three modules, the snow module allowing to separate snowfall from precipitation, the soil module that simulates the slow and quick runoff components ( $Q_{su}$  and  $Q_{fu}$ , respectively) and the routing module for flood simulation. Red arrows indicate input variables; black arrows indicate intermediate output variables; blue arrows indicate final output variables. The components  $Q_{fu}$  and  $Q_{su}$  are computed by using satellite  $P$ , soil moisture and TWSA data as input to the soil module. Please refer to text for symbols.

932



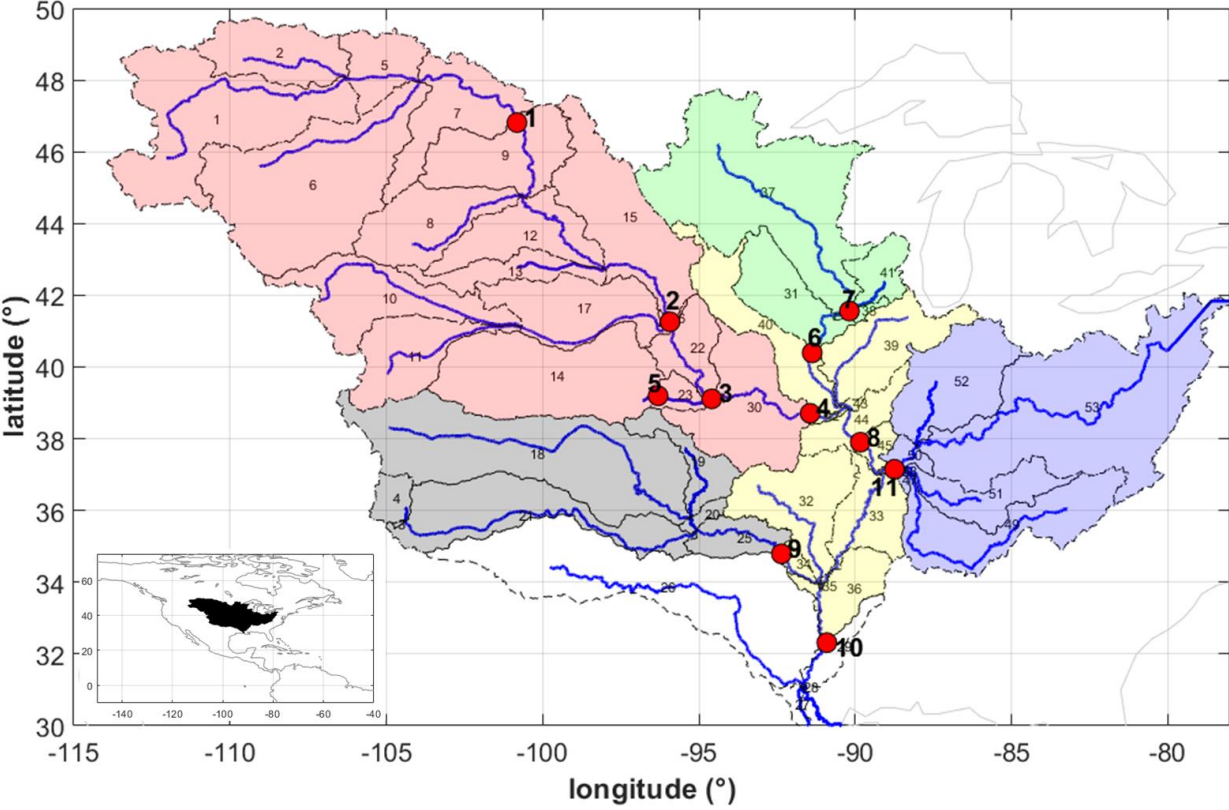
933

934

935 Figure 2. Processing steps of the STREAM v1.3 model.

936

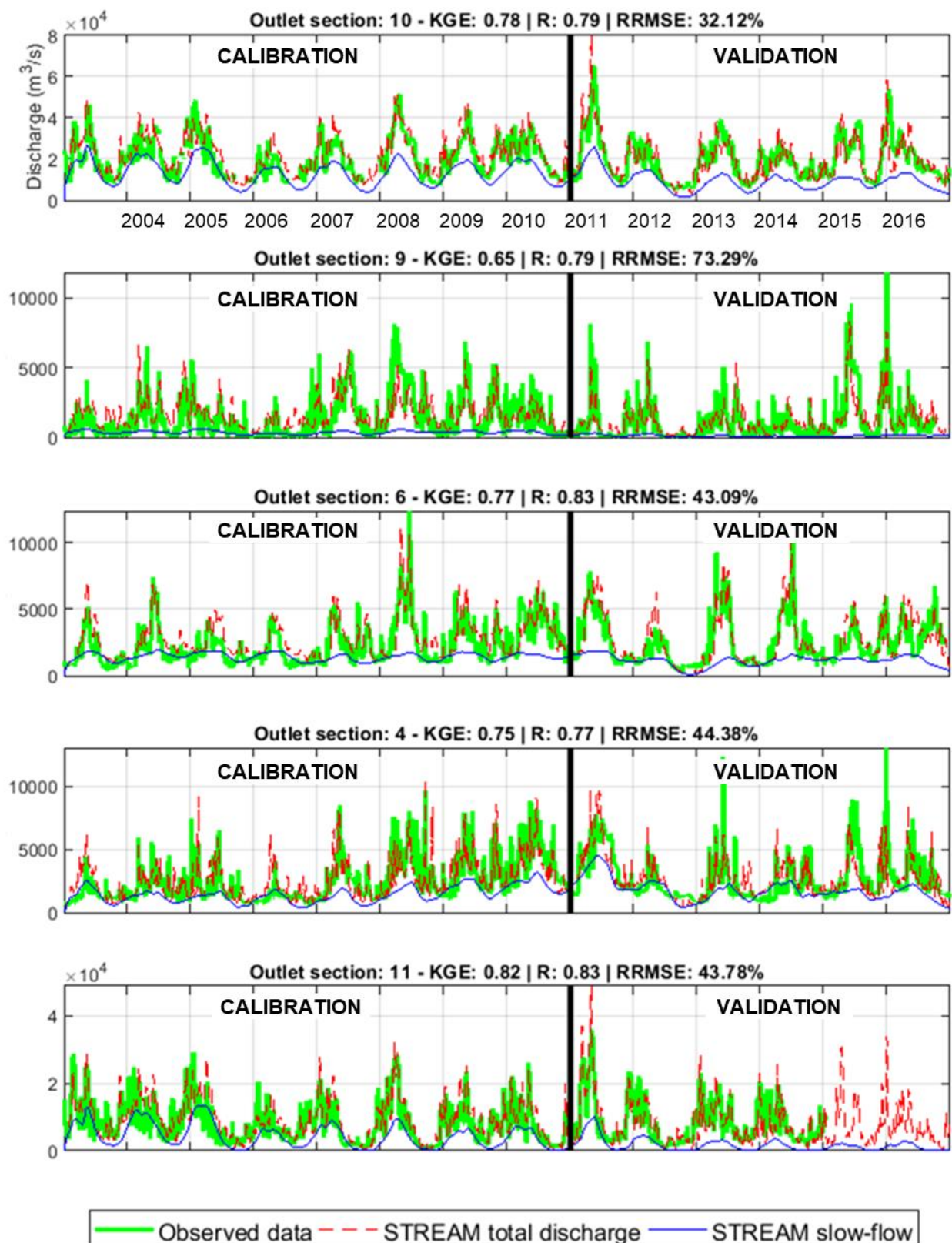
937



938

939 Figure 3. Mississippi sub-basin delineation. Red dots indicate the location of the discharge gauging  
940 stations; different colours identify different inner sections (and the related contributing sub-basins)  
941 used for the model calibration.  
942

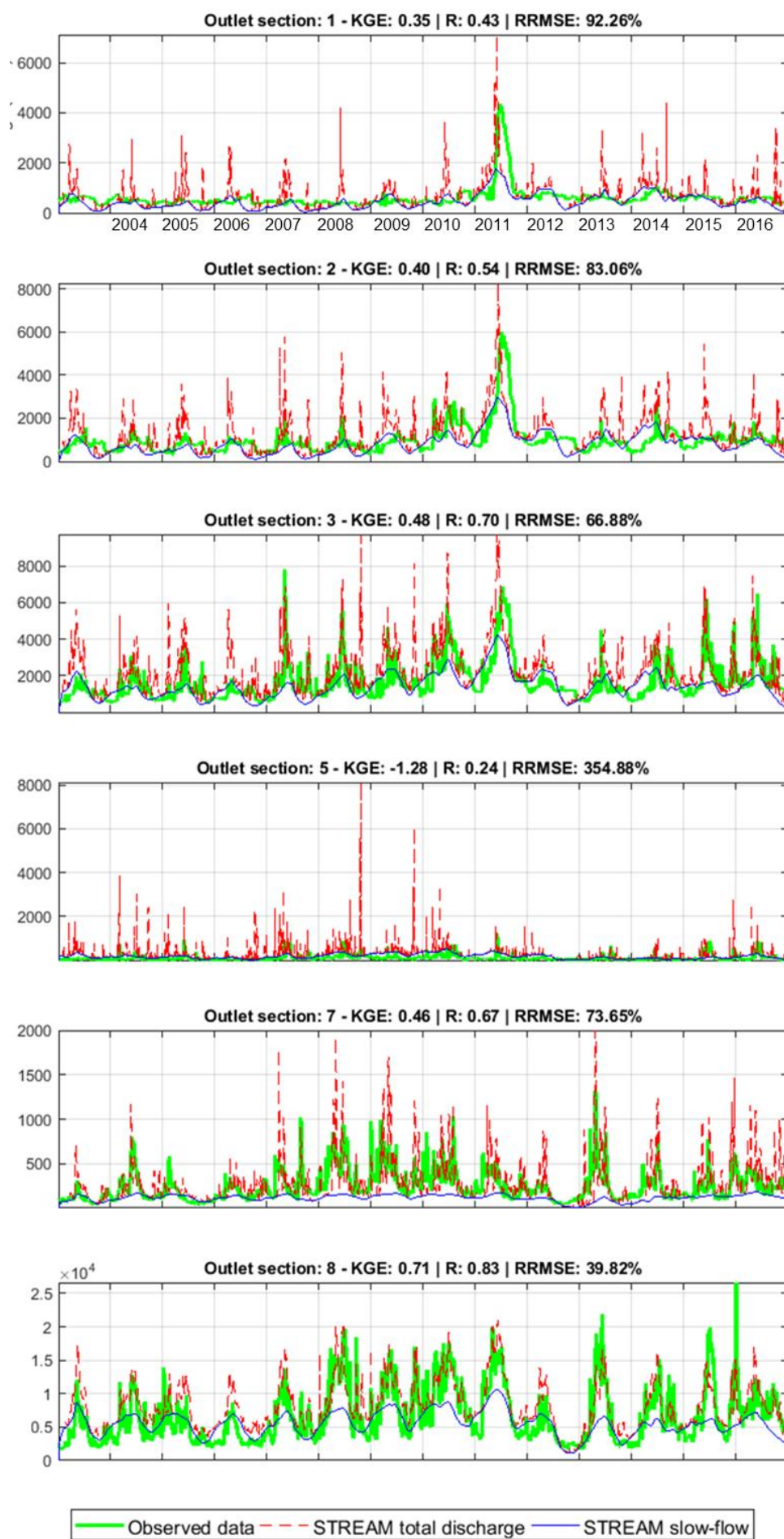




943

944 Figure 4. Comparison between observed and simulated river discharge time series over the five  
 945 calibrated sections over Mississippi river basin. Performance scores at the top of each plot refer to  
 946 the entire study period (2003–2016).

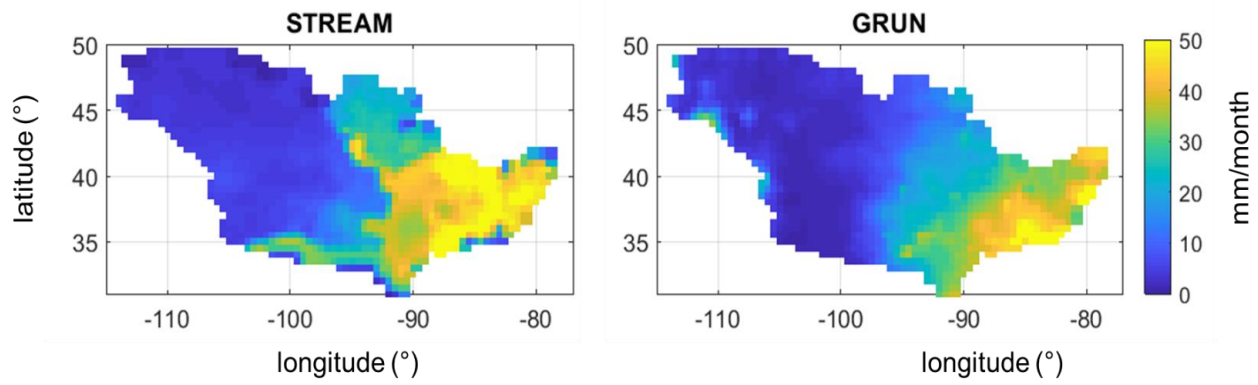
947





940  
941  
951  
952  
953  
954

Figure 5. Comparison between observed and simulated river discharge time series over the gauged sections not used in the calibration phase. Performance scores at the top of each plot refer to the entire study period (2003–2016).



955

956 Figure 6. Mississippi river basin: mean monthly runoff for the period 2003–2014 obtained by  
 957 STREAM v1.3 and GRUN models.

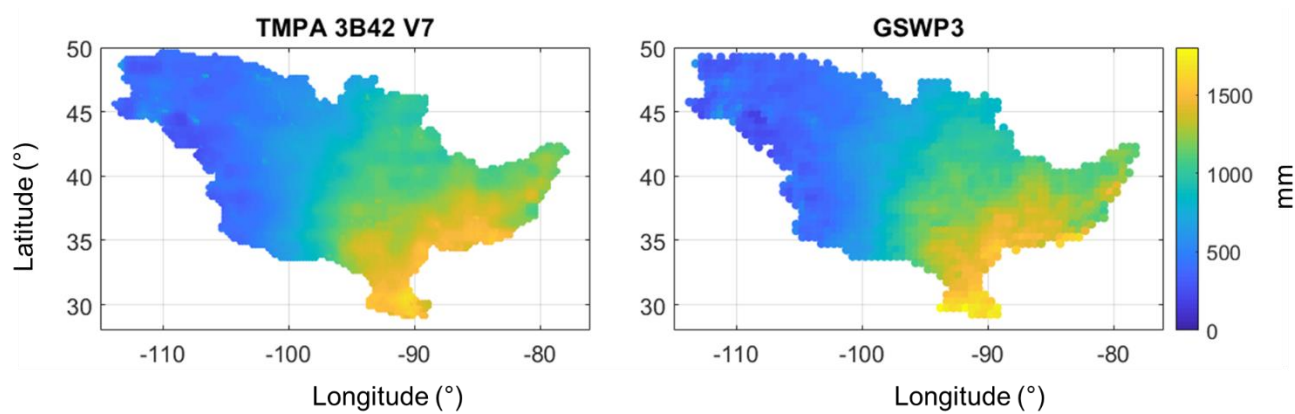
958

960    Table 1A. Description of STREAM v1.3 parameters, belonging module, variability range and unit.

Parameter	Description	Module	Range Variability	Unit
Cm	degree-day coefficient	Snow	0.1/24-3	[-]
$\alpha$	exponent of infiltration	Soil	1-30	[-]
T	characteristic time length	Soil	0.01-80	[days]
$\beta$	coefficient relationship slow runoff component and TWSA	Soil	0.1-20	[mm h-1]
m	exponent in the relationship between slow runoff component and TWSA	Soil	1-15	[-]
$\gamma$	parameter of GIUH	Routing	0.5-5.5	[-]
C	Celerity	Routing	1-60	[km h-1]
D	Diffusivity	Routing	1-30	[km2 h-1]

961

962



963

964 Figure S1. Mean annual precipitation data over the period 2003-2014 obtained by TMPA 3B42 V7  
 965 and GSWP3 datasets over the Mississippi river basin.

966